


การวิเคราะห์สมรรถนะของระบบเซลล์เชื้อเพลิงชนิดออกไซด์แข็งที่ป้อนเชื้อเพลิงด้วยเมทานอล



นายวิบูลย์ แสงทองกิจเจริญ

สถาบันวิทยบริการ

จุฬาลงกรณ์มหาวิทยาลัย

วิทยานิพนธ์นี้เป็นส่วนหนึ่งของการศึกษาตามหลักสูตรปริญญาวิศวกรรมศาสตรมหาบัณฑิต

สาขาวิชาวิศวกรรมเคมี ภาควิชาวิศวกรรมเคมี

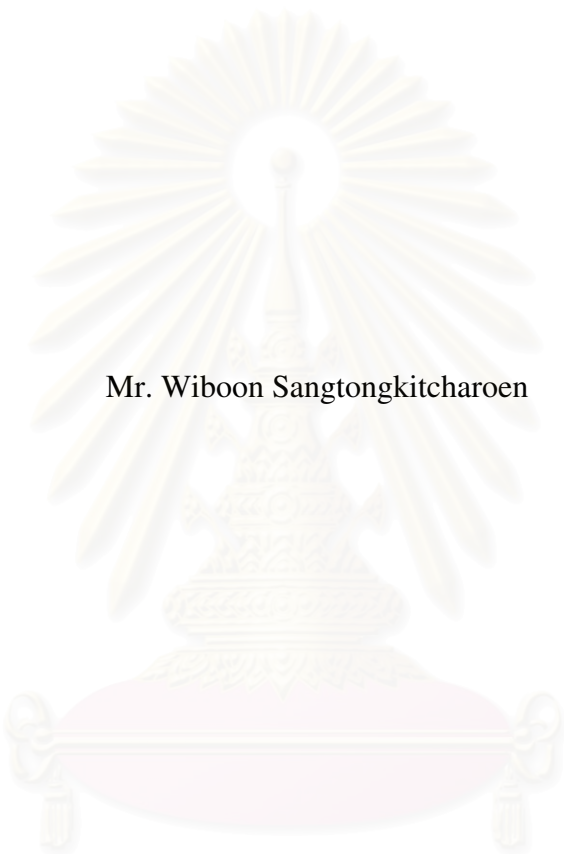
คณะวิศวกรรมศาสตร์ จุฬาลงกรณ์มหาวิทยาลัย

ปีการศึกษา 2548

ISBN 974-53-2811-1

ลิขสิทธิ์ของจุฬาลงกรณ์มหาวิทยาลัย

PERFORMANCE ANALYSIS OF SOLID OXIDE FUEL CELL SYSTEM
FUELED BY METHANOL



Mr. Wiboon Sangtongkitcharoen

สถาบันวิทยบริการ
จุฬาลงกรณ์มหาวิทยาลัย

A Thesis Submitted in Partial Fulfillment of the Requirements
For the Degree of Master of Engineering Program in Chemical Engineering
Department of Chemical Engineering
Faculty of Engineering
Chulalongkorn University
Academic Year 2005
ISBN 974-53-2811-1

Thesis Title PERFORMANCE ANALYSIS OF SOLID OXIDE FUEL
 CELL SYSTEM FUELED BY METHANOL


By Mr. Wiboon Sangtongkitcharoen

Field of Study Chemical Engineering

Thesis Advisor Associate Professor Suttichai Assabumrungrat, Ph.D.

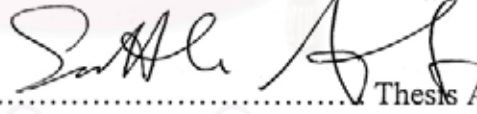
Thesis Co-advisor Navadol Laosiripojana, Ph.D.

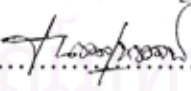
Accepted by the Faculty of Engineering, Chulalongkorn University in Partial
Fulfillment of the Requirements for the Master's Degree


..... Dean of the Faculty of Engineering
(Professor Direk Lavansiri, Ph.D.)

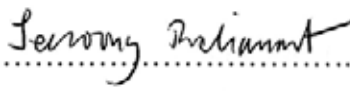
THESIS COMMITTEE

..... Chairman
(Associate Professor Prasert Pavasant,, Ph.D.)

..... Thesis Advisor
(Associate Professor Suttichai Assabumrungrat, Ph.D.)

..... Thesis Co-advisor
(Navadol Laosiripojana, Ph.D.)

..... Member
(Associate Professor Supakanok Thongyai, Ph.D.)

..... Member
(Assistant Professor Seeroong Prichanont, Ph.D.)

วิทยุль แสงทองกิจเจริญ: การวิเคราะห์สมรรถนะของระบบเซลล์เชื้อเพลิงชนิดออกไซด์แข็งที่ป้อนเชื้อเพลิงด้วยเมทานอล (PERFORMANCE ANALYSIS OF SOLID OXIDE FUEL CELL SYSTEM FUELED BY METHANOL) อ. ที่ปรึกษา: รศ.ดร. สุทธิชัย อัสสะบำรุงรัตน์, อ. ที่ปรึกษาร่วม: ดร. นวดล เหล่าศิริพจน์, 84 หน้า ISBN: 974-53-2811-1

วิทยานิพนธ์นี้ศึกษาเกี่ยวกับระบบเซลล์เชื้อเพลิงชนิดออกไซด์แข็ง (SOFC) ที่ใช้ตัวอิเล็กโตรไลต์แบบนำออกซิเจนไอออน (SOFC-O²⁻) และแบบนำโปรตรอน (SOFC-H⁺) โดยใช้เมทานอลเป็นเชื้อเพลิง การศึกษาแบ่งเป็นสามส่วน ประกอบด้วย การหาอัตราส่วนน้ำต่อเมทานอลป้อนเข้าที่เหมาะสมที่ป้องกันการเกิดคาร์บอนที่ขั้วแอโนดของเซลล์เชื้อเพลิง การเปรียบเทียบค่าประสิทธิภาพทางทฤษฎีของเซลล์เชื้อเพลิงที่ใช้ตัวอิเล็กโตรไลต์ต่างชนิดกันและมีรูปแบบการไหลที่แตกต่างกันคือ แบบไหลผสม (mixed flow, MF) และแบบปลั๊กโฟว์ (plug flow, PF) และการศึกษาข้อดีของการใช้เครื่องปฏิกรณ์แบบเมมเบรนที่ทำจากแพลลาเดียมในระบบของเซลล์เชื้อเพลิงชนิดออกไซด์แข็ง การคำนวณทางอุณหพลศาสตร์สำหรับการหาอัตราส่วนน้ำต่อเมทานอลป้อนเข้าที่เหมาะสมที่ป้องกันการเกิดคาร์บอนพบว่า เมื่อมีการเพิ่มอุณหภูมิในเซลล์เชื้อเพลิง ปริมาณน้ำที่ต้องการในระบบจะลดลง และสำหรับ SOFC-O²⁻ จะต้องการน้ำน้อยกว่า SOFC-H⁺ เนื่องจากจะมีน้ำที่เกิดจากปฏิกิริยาไฟฟ้าเคมีที่ขั้วแอโนดของเซลล์เชื้อเพลิง แต่ในแง่ของประสิทธิภาพของเซลล์นั้น เซลล์เชื้อเพลิงที่ใช้อิเล็กโตรไลต์แบบนำโปรตรอนจะมีประสิทธิภาพสูงกว่าอิเล็กโตรไลต์แบบนำออกซิเจน พบว่าค่าของประสิทธิภาพสูงสุดของเซลล์นั้นจะลดลงเมื่ออุณหภูมิสูงขึ้นและมีค่าเรียงลำดับดังนี้: SOFC-H⁺ (PF) > SOFC-O²⁻ (PF) > SOFC-H⁺ (MF) > SOFC-O²⁻ (MF) แต่สำหรับ SOFC-O²⁻ นั้นสามารถดำเนินการได้ในอัตราส่วนน้ำต่อเมทานอลที่ระดับน้อยที่สุดที่ป้องกันการเกิดคาร์บอนได้ แต่สำหรับ SOFC-H⁺ นั้นต้องใช้ที่ระดับ 1-1.5 เท่าของอัตราส่วนมวลสารสัมพันธ์ ถึงแม้ว่าสำหรับ SOFC-O²⁻ จะมีข้อดีในแง่ของความต้องการปริมาณน้ำป้อนเข้าที่น้อยกว่า แต่ SOFC-H⁺ ก็น่าสนใจมากกว่าในแง่ของประสิทธิภาพ นอกจากนี้ ในการศึกษาประโยชน์ของการใช้เครื่องปฏิกรณ์แบบเมมเบรนที่ทำจากแพลลาเดียมในระบบเซลล์เชื้อเพลิงพบว่าเพื่อให้ระบบสามารถผลิตพลังงานไฟฟ้าด้วยประสิทธิภาพเท่าเดิม ระบบที่ใช้เครื่องปฏิกรณ์แบบเมมเบรนจะใช้เซลล์เชื้อเพลิงขนาดเล็กกว่าแต่จะมีค่าใช้จ่ายเพิ่มเติมจากค่าเมมเบรนที่ต้องการเพิ่มในระบบ

ภาควิชา.....วิศวกรรมเคมี
สาขาวิชา.....วิศวกรรมเคมี
ปีการศึกษา.....2548

ลายมือชื่อนิสิต.....
ลายมือชื่ออาจารย์ที่ปรึกษา.....
ลายมือชื่ออาจารย์ที่ปรึกษาร่วม.....

4770456821 : MAJOR CHEMICAL ENGINEERING

KEY WORDS: SOLID OXIDE FUEL CELL, METHANOL, CARBON FORMATION, THEORETICAL PERFORMANCE, PALLADIUM MEMBRANE REACTOR

WIBOON SANGTONGKITCHAROEN : PERFORMANCE ANALYSIS OF SOLID OXIDE FUEL CELL SYSTEM FUELED BY METHANOL. THESIS ADVISOR: ASSOCIATE PROFESSOR SUTTICHAJ ASSABUMRUNGRAT, Ph.D., THESIS COADVISOR: NAVADOL LAOSIRIPOJANA, Ph.D., 84 pp. ISBN: 974-53-2811-1

This thesis investigates performance of Solid Oxide Fuel Cell (SOFC) system fed by methanol. Two types of solid electrolyte, i.e. oxygen-ion (SOFC-O²⁻) and proton-conducting (SOFC-H⁺) electrolyte are considered. The thesis consists of three main parts, firstly, determination of inlet steam: methanol ratio at boundary of carbon formation, secondly, comparison of theoretical performance between two types of electrolyte and different of flow pattern (i.e. mixed flow (MF) and plug flow (PF)) and, lastly, investigation on benefit of application of palladium membrane reactor in SOFC-O²⁻ system. It was found from the thermodynamic calculation that the minimum steam: methanol ratio for which carbon formation is thermodynamically unfavoured decreases with increasing temperature. Comparison between the two types of electrolyte reveals that the SOFC-O²⁻ requires lower steam for the prevention for carbon formation due to the water formed by the electrochemical reaction at the anode side. In the efficiency point of view SOFC-H⁺ shows higher efficiency than SOFC-O²⁻. It is demonstrated that the maximum efficiencies decrease with increasing temperature and follow the sequence: SOFC-H⁺ (PF) > SOFC-O²⁻ (PF) > SOFC-H⁺ (MF) > SOFC-O²⁻ (MF). The corresponding inlet steam: methanol ratios are at the carbon formation boundary for the SOFC-O²⁻ electrolyte, but are about 1.3–1.5 times the stoichiometric ratio for the SOFC-H⁺. Although the benefit from the lower steam requirement is realized for the SOFC-O²⁻, the use of the SOFC-H⁺ electrolyte in the SOFCs is more promising in the theoretical consideration. Finally, it was found that for the SOFC system equipped with Palladium membrane reactor, at the same electrical efficiency of the conventional SOFC system the system requires smaller SOFC stack; however, additional cost of the membrane is required.

Department Chemical Engineering.....

Field of Study Chemical Engineering.....

Academic year 2005.....

Student's signature Wiboon Sangtongkitcharoen

Advisor's signature Suttichai Assabumrungrat

Co-advisor's signature Navadol Laosiripojana

ACKNOWLEDGEMENTS

The author would like to express his sincere gratitude and appreciation to his advisor, Associate Professor Suttichai Assabumrungrat, for his invaluable suggestions, stimulating, useful discussions throughout this research and devotion to revise this thesis otherwise it can not be completed in a short time. Without the comments from his co-advisor Dr. Navadol Laosiripojana of The Joint Graduate School of Energy and Environment, King Mongkut's University of Technology Thonburi, this work would never have been achieved. In addition the author would also be grateful to Associate Professor Prasert Pavasant, as the chairman, Associate Professor Supakanok Thongyai and Assistant Professor Seeroong Prichanont as the members of the thesis committee. The financial support from the Thailand Research Fund and Chulalongkorn University Graduate Scholarship Commemorating the 72nd Anniversary of H.M. King RAMA IX is gratefully acknowledged.

Most of all, the author would like to express his highest gratitude to his parents who always pay attention to his all times for suggestions and have provided his support and encouragement. The most success of graduation is devoted to his parents.

Finally, the author wishes to thank the members of the Center of Excellence on Catalysis and Catalysis Reaction Engineering, Department of Chemical Engineering, Faculty of Engineering, Chulalongkorn University for their assistance.

สถาบันวิทยบริการ
จุฬาลงกรณ์มหาวิทยาลัย

CONTENTS

	PAGE
ABSTRACT (IN THAI).....	iv
ABSTRACT (IN ENGLISH).....	v
ACKNOWLEDGEMENTS.....	vi
CONTENTS.....	vii
LIST OF TABLES.....	x
LIST OF FIGURES.....	xi
NOMENCLATURE.....	xiii
CHAPTER	
I INTRODUCTION.....	1
II THEORY.....	4
2.1 Principle of fuel.....	4
2.2 Solid Oxide Fuel Cell (SOFC).....	10
2.3 Solid Oxide Fuel Cell System.....	14
2.4 Palladium membrane.....	15
III LITERATURE REVIEWS.....	17
3.1 Fuel cell.....	17
3.2 Methanol steam reforming.....	17
3.3 Coke formation.....	18
3.4 Fuel cell system analysis.....	20
3.5 Palladium membrane.....	22
IV DETERMINATION OF BOUNDARY OF CARBON FORMATION FOR SOFC WITH DIFFERENT ELECTROLYTE TYPE.....	23
4.1 Calculation of the converted mole of methanol steam reforming.....	24
4.2 Determining of boundary of carbon formation.....	27
4.3 Results and discussion.....	29
4.3.1 Effect of the extent of hydrogen consumption on anode components.....	29
4.3.2 Effect of hydrogen consumption on carbon formation.....	31

CONTENTS

CHAPTER	PAGE
4.4 Conclusion.....	35
V THEATRICAL PERFORMANCE ANALYSIS OF SOFC WITH DIFFERENT ELECTROLYTE TYPE.....	36
5.1 Electrochemical reaction.....	37
5.2 Theoretical performance.....	37
5.3 Results and discussion.....	40
5.3.1 Effect of fuel utilization on theoretical performance.....	40
5.3.2 Effect of inlet mole ratio on theoretical performance.....	43
5.3.3 Maximum efficiency.....	45
5.4 Conclusions.....	47
VI BENEFIT OF INCORPORATING PALLADIUM MEMBRANE REACTOR IN SOLID OXIDE FUEL CELL SYSTEM.....	48
6.1 SOFC model.....	49
6.2 Solid oxide fuel cell system.....	50
6.2.1 Reformer.....	52
6.2.2 Solid Oxide Fuel Cell.....	53
6.2.3 Afterburner.....	53
6.2.4 Compression unit.....	53
6.2.5 Net heat.....	54
6.3 Palladium membrane reactor.....	55
6.4 Results and discussion.....	56
6.4.1 Performance of SOFC unit.....	56
6.4.2 Performance comparison between with and without membrane reactor.....	58
6.4.2.1 Effect of operating pressure of membrane reactor on hydrogen recovery.....	58
	59

CONTENTS

CHAPTER	PAGE
6.4.2.2 Effect of hydrogen recovery on performance of SOFC unit.....	59
6.4.2.3 Benefit from the use of membrane reactor in the SOFC system.....	60
6.5 Conclusion.....	63
VII CONCLUSIONS AND RECOMMENDATIONS.....	64
7.1 Conclusions.....	64
7.2 Recommendations.....	65
REFERENCES.....	66
APPENDICES.....	72
APPENDIX A: SELECTED THERMODYNAMIC DATA.....	73
APPENDIX B: DETERMINING GIBBS ENERGY.....	74
B1 Determining Gibbs energy (G).....	74
B2 Determining the equilibrium constant (K).....	74
APPENDIX C: NEWTON'S METHOD.....	76
APPENDIX D: THE CALCULATION OF SOLID OXIDE FUEL CELL SYSTEM.....	78
APPENDIX E: PALLADIUM MEMBRANE REACTOR.....	81
APPENDIX F: LIST OF PUBLICATIONS.....	83
VITA.....	84

LIST OF TABLES

TABLE	PAGE
2.1 Summary characteristics of different types of fuel cells.....	9
6.1 Operating condition.....	54
6.2 Results of simulation	62
A1 Heat capacities (C_p)	73
A2 Heat of formation (H_f), and entropy (S^0).....	73
D1 Resistivity and thickness of cell component.....	78
D2 Constant used for the cathode and anode polarization resistance...	79
D3 Total activation overpotential using Achenbach at 3000A/m^2 from literature.....	80
E1 Regressed parameter for the diffusion of hydrogen through Pd membrane.....	82

LIST OF FIGURES

FIGURE	PAGE
2.1 Simple Fuel cell.....	4
2.2 Alkaline Fuel Cell (AFC).....	6
2.3 Proton Exchange Membrane (PEM).....	6
2.4 Phosphoric Acid Fuel Cell (PAFC).....	8
2.5 Molten Carbonate Fuel Cell (MCFC).....	8
2.6 Solid Oxide Fuel Cell (SOFC).....	8
2.7 Oxygen ion-conducting electrolyte.....	11
2.8 Proton-conducting electrolyte.....	11
2.9 Configurations of various SOFC modes (a) ER-SOFC, (b) IIR-SOFC and (c) DIR-SOFC.....	12
2.10 Solid Oxide Fuel Cell system.....	14
2.11 Mechanism of Hydrogen diffusion in palladium membrane.....	16
4.1 Influence of the extent of the electrochemical reaction of hydrogen on moles of components at the anode side (oxygen ion-conducting electrolyte, $a = 1$ mol, $b = 1$ mol, $P = 1$ atm and $T = 1173$ K).....	30
4.2 Influence of the extent of the electrochemical reaction of hydrogen on moles of components in the anode side (proton-conducting electrolyte, $a = 1$ mol, $b = 1$ mol, $P = 1$ atm and $T = 1173$ K).....	30
4.3 Effect of inlet H ₂ O: MeOH ratio on each component mole at the anode side (oxygen ion-conducting electrolyte, $a = 1$ mol, $P = 1$ atm, $T = 1173$ K): (a) $c = 0$ mol, and (b) $c = 1.5$ mol.....	33
4.4 Influence of the extent of the electrochemical reaction of hydrogen on the requirement of inlet H ₂ O: MeOH ratio at different operating temperatures (oxygen ion-conducting electrolyte, $a = 1$ mol, $P = 1$ atm).....	34
4.5 Influence of the extent of the electrochemical reaction of hydrogen on the requirement of inlet H ₂ O: MeOH ratio at different operating temperatures (proton-conducting electrolyte, $a = 1$ mol, $P = 1$ atm).....	34
5.1 Performance of SOFC-O ²⁻ and SOFC-H ⁺ operated under plug flow (PF) and mixed flow (MF): (a) efficiency; (b) electromotive force (inlet H ₂ O: MeOH = 1, $T = 1173$ K, $P = 1$ atm).....	42

FIGURE	PAGE
5.2 Influence of inlet H ₂ O: MeOH ratio on SOFC performance at fuel utilization of 90% (solid line) and 99% (dashed line): (a) efficiency; (b) electromotive force ($T = 1173 \text{ K}$, $P = 1 \text{ atm}$).....	44
5.3 Maximum efficiency of different SOFCs at different operating temperatures ($P = 1 \text{ atm}$).....	46
5.4 Operating conditions corresponding to those in Fig. 5.5, at maximum efficiency ($P = 1 \text{ atm}$).....	46
6.1 A conventional solid oxide fuel cell system.....	51
6.2 A solid oxide fuel cell system integrated with a membrane separation unit.....	52
6.3 Performance characteristics for comparison effect of fuel utilization at inlet H ₂ O: MeOH = 1 and $T = 1173 \text{ K}$ (Solid lines represent power density, Dash lines represent voltage).....	57
6.4 Performance characteristics for comparison effect of fuel cell temperature at inlet H ₂ O: MeOH = 1 and $U_f = 80 \%$	57
6.5 Performance of SOFC at maximum power density for comparison effect of fuel utilization and operating temperature at inlet H ₂ O: MeOH = 1 (Solid lines represent efficiency, Dash lines represent power density).....	58
6.6 Effect of pressure on hydrogen recovery by Pd membrane at inlet H ₂ O: MeOH = 1, $U_f = 80 \%$ and $T = 1173 \text{ K}$	59
6.7 Performance characteristics for comparison effect of hydrogen recovery at inlet H ₂ O: MeOH = 1, $U_f = 80 \%$, $T = 1173 \text{ K}$ (Dashed line represents conventional SOFC system and solid lines represent SOFC system plus separation unit).....	60
6.8 Effect of hydrogen recovery on reduction of fuel cell area (solid line) and membrane area (dashed line) at inlet H ₂ O: MeOH = 1, $U_f = 80 \%$ and $T = 1173 \text{ K}$	63
D1 Total activation overpotential using Achenbach at current density 3000 A/m^2	78

NOMENCLATURE

a	inlet moles of Fuel	[mol]
A	Area	[m ²]
b	inlet moles of water	[mol]
c	extent of the electrochemical reaction of hydrogen	[mol]
E_0	Electromotive force	[V]
E_D	Activation energy for diffusion through membrane	[kJ mol ⁻¹]
Eff	Efficiency	[%]
f	Volumetric flow rate	[m ³ s ⁻¹]
F	Faraday's Constant (96485.3383)	[c mol ⁻¹]
G	Gibb Free Energy	[kJ]
H	Enthalpy	[kJ]
i	Current density	[A cm ⁻²]
k	Hydrogen perability of metal	[mol (m ³ s pa ^{0.5}) ⁻¹]
K_i	Equilibrium constant of reaction i	[kPa ⁻¹]
K_s	Sieverts constant	[mol (m ³ pa ^{0.5}) ⁻¹]
n_i	Number of moles of component i	[mol]
N_i	Molar flux of hydrogen	[mol m ⁻²]
P	Total pressure	[atm]
p_i	Partial pressure of component i	[kPa]
P_{com}	Power in compression unit	[kW]
q	Electrical charge	[mol]
Rec	Hydrogen recovery	[%]
Q_0	pre-exponential constant for membrane permeability	[mol (m s Pa ^{-0.5}) ⁻¹]
Q_i	Power consumption in each unit	[kW]
R	Universal Gas Constant (8.31447)	[J g mol K]
R_j	Resistance	[Ω]
T	Absolute temperature	[K]
U_f	Fuel Utilization	[%]
V	Operating Voltage	[V]
W	Maximum electrical work	[W]
x_i	Converted moles associated with reaction i	[mol]

$-\Delta H^0$ Low Heating Value (LHV) [kW]

Greeks letters

α_c	carbon activity	[-]
φ_i	Potential	[V]
η	Overpotential	[V]
δ	Thickness	[m]
ρ	resistivity	[Ω m]

Subscripts

<i>a</i>	Anode
<i>Act</i>	Activation
<i>c</i>	Cathode
<i>Conc</i>	Concentration
<i>FC</i>	Fuel cell
<i>Mem</i>	Membrane
<i>Ohm</i>	Ohmic
<i>RF</i>	Reformer

สถาบันวิทยบริการ
จุฬาลงกรณ์มหาวิทยาลัย

CHAPTER I

INTRODUCTION

Fuel cell is considered as an efficient electrical power generator compared to conventional heat engines, steam and gas turbine, and combined cycles. Among the various types of fuel cell, solid oxide fuel cell (SOFC) has attracted considerable interest as it offers the widest range of applications, flexibility in the choice of fuel, high system efficiency and possibility of operation with an internal reformer.

The major source of fuel for fuel cells is hydrogen which can be derived from many hydrocarbon-based processes and electrolysis of water. Nevertheless, the other fuels such as methane, methanol, ethanol, gasoline and oil derivatives are also possible fuel for use in for SOFC. Douvartzide *et al.* (2003b) applied a thermodynamic analysis to evaluate the flexibility of different fuels i.e., methane, methanol, ethanol and gasoline, for SOFC. The results obtained in terms of electromotive force output and efficiency show that ethanol and methanol are very promising alternatives to hydrogen. Methanol is a preferable choice with respect to its availability, high energy density and ready storage and distribution.

Although the steam reforming of methanol for hydrogen production is possible from a thermodynamic point of view, a major consideration is carbon formation in the system. Appropriate operating conditions must be carefully selected to avoid damage from carbon formation such as catalyst deactivation in the reformer or anode deactivation in a SOFC with internal reformer. The formation of carbon leads to low of system performance and poor durability. There have many methods proposed for controlling this problem, for example the addition of alkalis such as potassium can accelerate the reaction of carbon with steam and also neutralize the acidity of the catalyst support, hence reducing carbon deposition (Finnerty *et al.*, 1998). For the steam reforming, addition of extra steam to the feed is a conventional approach to avoid carbon deposition. Selection of a suitable steam/hydrocarbon ratio becomes an important issue. Carbon formation can occur when the SOFC is operated at low steam/hydrocarbon ratio. However, use of high steam/hydrocarbon ratio is

unattractive as it lowers the electrical efficiency of the SOFC by steam dilution of fuel and the system efficiency (Park, *et al.*, 2000). Therefore the information on boundary of carbon formation is useful for safe operation of reformer or SOFC.

In operation, the SOFC can use either an oxygen ion-conducting electrolyte (SOFC-O²⁻) or a proton-conducting electrolyte (SOFC-H⁺). Most current researches have been focusing on SOFC-O²⁻ rather than the other. Thermodynamic analysis reveals that the SOFC-H⁺ shows higher theoretical efficiency for the conversion of chemical energy to electrical power than the SOFC-O²⁻ for system fed by hydrogen (Brown *et al.*, 2001) and methane (Demin *et al.*, 2002). However, their studies were based on the same steam/fuel ratio. It was reported that the steam requirement for SOFC-O²⁻ is less than that of the SOFC-H⁺ (Assabumrungrat *et al.*, 2004). Therefore, it is interesting to compare theoretical performances of SOFCs with different electrolyte when the difference in steam requirement is taken into account. Thus information is important for focusing on the future of SOFC development.

In generally SOFCs system consists of preheater, reformer, SOFC and burner. Most fuel cells need to convert a hydrogen primary fuel into a hydrogen-rich gas required for the electrochemical reaction on the anode side. The methanol feed is converted to hydrogen with endothermic steam reforming reactions in the reformer. In the most common case of a reformer, heat needs to be available to drive the steam reforming reaction. One method of achieving this is to feed the exhaust gases from the anode and cathode into a burner where the excess fuel is combusted. The heat generated in the burner can then be used to preheat both the steam and the fuel, and provide the heat needed in the reformer (Aguiar *et al.*, 2002; Aguiar *et al.*, 2004). Such operation is of concern for the system design which is expected to lead to an increase in efficiency.

A number of works have been devoted on studying SOFC system design and balance of plant (i.e. Monanteras and Frangopoulos, 1999; Koh *et al.*, 2005). It has been demonstrated that hydrogen concentration in feed influences SOFC performance (Chan *et al.*, 2005). In particular, stack power density should be higher at high hydrogen partial pressure feed. A palladium membrane reactor has been applied to a number of hydrogen-generating reactions (i.e. Jarosch *et al.*, 2001). Removal of

hydrogen from the reaction zone can improve the extent of reaction and pure hydrogen can be obtained. It is, therefore, an interesting topic to find out whether the replacement of a conventional reformer by the membrane reactor in the SOFC system could improve system performance. The stack power density is expected to be higher; however, the system would require additional expensive palladium membranes and operating cost in the operation.

Objective of this work

1. To find inlet steam per methanol ratios at the boundary of carbon formation for SOFC with oxygen ion-conducting electrolyte (SOFC-O²⁻) and SOFC with proton-conducting electrolyte (SOFC-H⁺).
2. To compare theoretical performance of SOFC-O²⁻ and SOFC-H⁺ when the different steam requirement is taken into account.
3. To investigate the benefit from integration of a palladium membrane reactor in the SOFC system.

CHAPTER II

THEORY

2.1 Principle of fuel cell

A fuel cell is an electrochemical device that generates electrical power with high efficiency. Fuel cell technology is based upon the simple combustion reaction given by Eq. 2.1

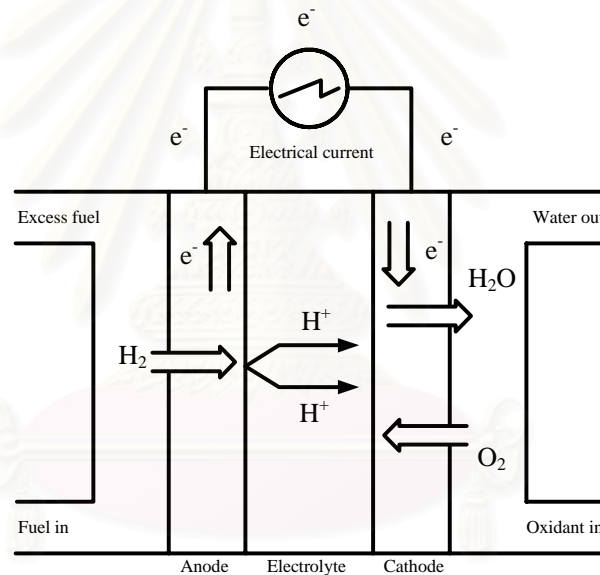


Fig 2.1 Simple Fuel cell

A fuel cell consists of an electrolyte and two electrodes (anode and cathode). The early fuel cells are not attractive as they have very high resistance through the electrolyte as a result of the long distance between the electrodes and very small contact area between the electrolyte, the electrode and the gas fuel. Novel fuel cells have been designed to avoid these problems. A design solution includes manufacturing a flat plate for the electrodes with an electrolyte of very small thickness between two electrodes. This design gives the maximum area of contact

between the electrodes, electrolyte and gas thus increasing the efficiency and current of fuel cell.

Batteries and fuel cells are similar in the sense that both of them efficiently convert chemical energy directly into electricity. The difference is that in batteries the chemical energy has to be stored prior to being consumed and, upon being used up, the battery must be recharged, while a fuel cell does not require. In theory, a fuel cell can produce electricity as long as fuel is constantly supplied. The hydrogen feed can be supplied from a variety of substances if a “fuel reformer” is added to the fuel cell system. Therefore, hydrogen can be obtained from hydrocarbon fuel such as natural gas or alcohols such as methanol or ethanol

Fuel cells can be classified by type of electrolyte used in the cell. The following fuel cells are listed in the order of operating temperature (Larinie *et al.*, 2000; Hirschenhofs *et al.*, 1998):

1. Alkaline Fuel Cell (AFC)
2. Proton Exchange Membrane (PEM)
3. Phosphoric Acid Fuel Cell (PAFC)
4. Molten Carbonate Fuel Cell (MCFC)
5. Solid Oxide Fuel Cell (SOFC)

Table 2.1 summarizes general characteristics of the different fuel cells and following paragraphs provide brief descriptions.

Alkaline Fuel Cell (AFC)

This type of fuel cell was employed as the on-board power system for the Apollo lunar program. Its success has stimulated the restart of the interest in the fuel cell technology. In this type, a concentrated solution of potassium hydroxide acts as electrolyte and coolant. It conducts hydroxyl ions (OH⁻) from the cathode to the anode. The disadvantage of this fuel cell type is that it is easily poisoned by carbon dioxide (CO₂) because it reacts with hydroxyl ions (OH⁻) to form carbonate ions (CO₃²⁻), destroying the electrolyte. It is necessary to purify both hydrogen and oxygen

used in the cell, this purification process is costly. Susceptibility to poisoning also affects the cell's lifetime, further adding to cost.

Proton Exchange Membrane (PEM) Fuel Cells or Polymer Electrolyte Membrane Fuel Cell

Their advantages are low weight and volume, compared with others. The electrolyte is solid polymer and porous carbon electrodes containing a platinum catalyst. To work, the electrolyte membrane must be saturated with water to conduct protons from the anode side to the cathode side. This limits the available span of operation temperatures; typical temperature is 353 K. Low temperature operation allows them to start quickly (less warm-up time). However, a highly active noble-metal catalyst (typically platinum) must be used to separate the hydrogen's electron and proton, adding the system's cost. The platinum catalyst is also extremely sensitive to carbon monoxide (CO) poisoning, making it necessary to employ an additional reactor to reduce CO in the fuel gas if hydrogen is derived from an alcohol or hydrocarbon fuel. Developers are currently exploring platinum/ruthenium (Pt/Ru) catalysts that are more resistive to CO.

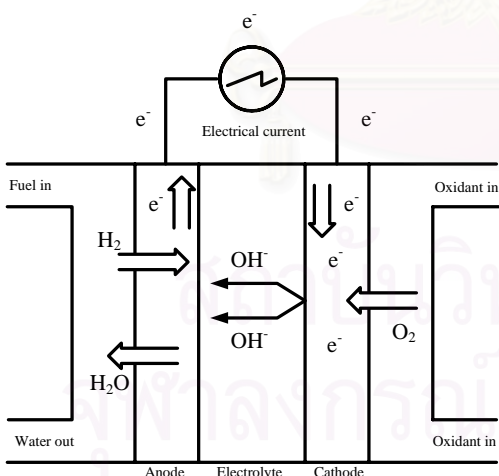


Fig.2.2 Alkaline Fuel Cell (AFC)

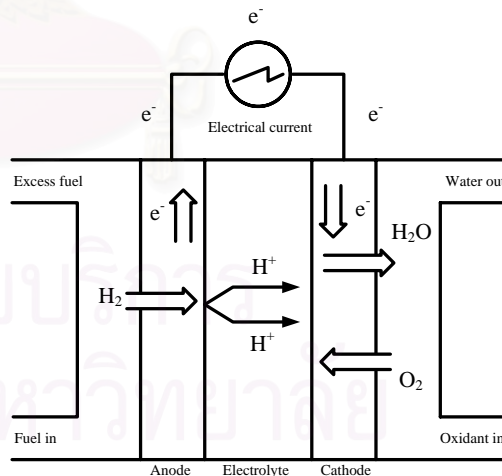


Fig.2.3 Proton Exchange Membrane (PEM)

Phosphoric Acid Fuel Cell (PAFC)

PAFC was the first commercial fuel cell found its application on widespread terrestrial use. PAFC uses ortho-phosphoric acid, H_3PO_4 , for its electrolyte. Anode and cathode are made of graphite with a platinum catalyst, and operating temperature is 423-493 K. PAFC is more tolerant of impurities in the fuel than PEM, which is easily “poisoned” by carbon monoxide – carbon monoxide binds to the platinum catalyst at the anode, thus decreasing the fuel cell’s efficiency. PAFC is less powerful than other fuel cells, given the same weight and volume. As the result, these fuel cells are typically large and heavy.

Molten Carbonate Fuel Cell (MCFC)

MCFC has an electrolyte made of a molten carbonate salt such as KLiCO_3 . The anode is porous nickel while the cathode consists of nickel oxide (NiO) and lithium oxide (Li_2O) because they operate at extremely high temperatures of 923 K or above, non-precious metals can be used as catalysts, thus reducing costs. Unlike other fuel cells, MCFC does not require an external reformer to convert more energy-dense fuels to hydrogen. Due to the high temperatures at which they operate, these fuels are converted to hydrogen within the fuel cell itself by a process called “internal reforming”, which also reduce cost. In MCFC it is necessary to supply both oxygen and carbon dioxide to the cathode to produce carbonate ions (CO_3^{2-}) which are transported through the electrolyte. If natural gas is used, carbon dioxide is also produced but at the anode side. It can be separated from the anode exhaust and fed to the cathode, which is shown in the diagram at below. The salt melt, saturated with oxygen and carbon dioxide, is extremely corrosive. This limits lifespan of the cell.

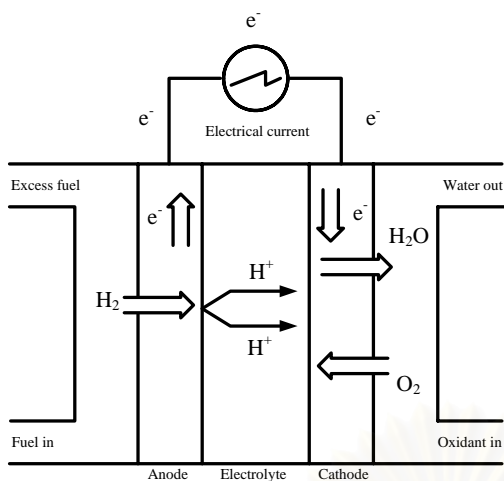


Fig.2.4 Phosphoric Acid Fuel Cell
(PAFC)

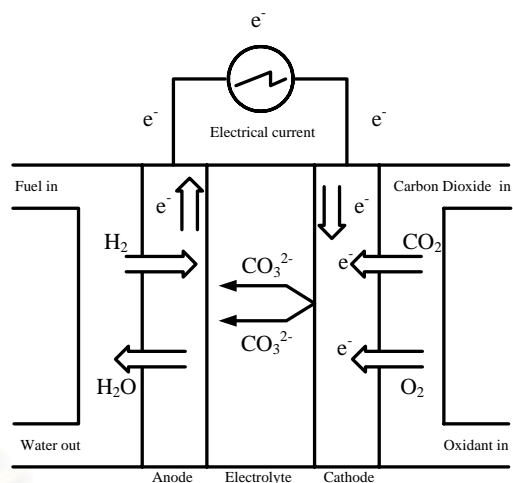


Fig.2.5 Molten Carbonate Fuel Cell
(MCFC)

Solid Oxide Fuel Cell (SOFC)

SOFC is operated in the region of high temperature. This means that high reaction rates can be achieved without expensive catalyst. Moreover fuel can be used directly or “internally reformed” within the fuel cell, without the need for the separate unit. SOFC is described in more detail in next section.

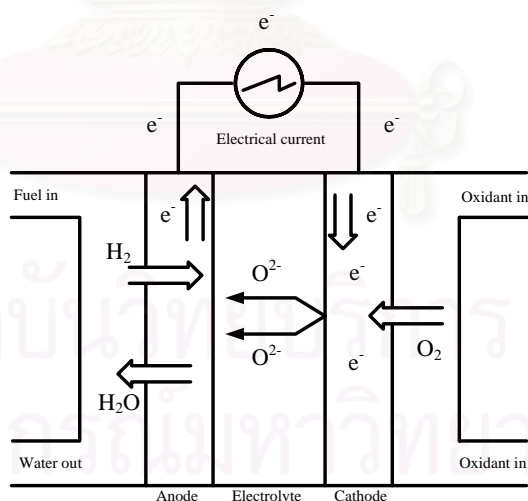


Fig.2.6 Solid Oxide Fuel Cell (SOFC)

Table 2.1 Summary characteristics of different types of fuel cells (Larinie *et al.*, 2000; Aguiar, 2002)

Fuel cell	Temperature (K)	Electrolyte	Cathode catalyst	Anode catalyst	Mobile ion	Reformer	Application	Advantage	Disadvantage
AFC	323-363	• Potassium hydroxide	• Pt/Au • Pt • Ag	• Pt/Au • Pt • Ag	• OH ⁻	• ER	• Military • Space	• Cathode reaction faster in alkaline electrolyte so high performance	• Expensive removal of CO ₂ from fuel and air streams required
PEM	323-398	• Solid proton-conducting polymer	• Pt	• Pt • Pt/Ru	• H ⁺	• ER	• Electric utility • Portable power • Transportation	• Solid electrolyte reduces corrosion & management problems • Quick start-up	• Low temperature requires expensive catalysts • High sensitivity to fuel impurities
PAFC	463-483	• Ortho-phosphoric acid	• Pt/Cr/Co • Pt/Ni	• Pt	• H ⁺	• ER	• Electric utility • Transportation	• Up to 85% efficiency in cogeneration of electricity and heat • Can use impure H ₂ as fuel	• Requires platinum catalyst • Low current and power • Large size/weight
MCFC	873-973	• Lithium • Potassium carbonate mixture	• Li/NiO	• Ni • Ni/Cs	• CO ₃ ²⁻	• ER • IR	• Electric utility	• High efficiency • Can use a variety of fuels and catalysts	• High temperature enhances corrosion and breakdown of cell components
SOFC	773-1373	• Stabilised zirconia oxide	• LaSrMnO ₃	• Ni/ZrO ₂	• O ²⁻ • H ⁺	• ER • IR	• Electric utility	• High efficiency • Can use a variety of fuels and catalysts • Solid electrolyte reduces corrosion • Quick start	• High temperature enhances corrosion and breakdown of cell components

2.2 Solid Oxide fuel cell (SOFC)

SOFC consists of two porous ceramic electrodes, the anode and the cathode, separated by a solid ceramic electrolyte. Typical SOFC materials are stabilized zirconia (Y_2O_3 stabilized ZrO_2) for electrolyte, nickel/zirconia (Ni-ZrO_2) cermet for anode, and doped lanthanum manganite (Sr-doped LaMnO_3) for cathode (Yamamoto, 2000; Badwal and Foger., 1996). It operates at high temperature (773-1373 K) and atmospheric or elevated pressure. High temperature operation removes the need for precious-metal catalyst, thereby reducing cost. It also allows SOFC to reform fuels internally, which enables the use of a variety of fuels and reduces the cost and size associated with addition of a reformer to the system. SOFC is also the most sulfur resistant fuel cell type; they can tolerate several orders of magnitude of sulfur higher than other fuel cell types. In addition, they are not poisoned by carbon monoxide. Their efficiency could be up to 80-85 %

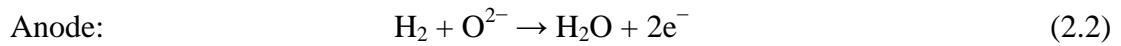
Advantages of Solid Oxide Fuel Cell (SOFC)

- SOFC is the most efficient fuel cell for electricity generation among the fuel cells currently being developed world wide.
- The solid electrolyte eliminates problems of electrolyte containment and migration and allows for design, that utilizes the electrolyte as a part of the structural members of the cells
- SOFC can be operated at high temperature. That allows for internal reforming of gases fuel within the cells, promotes rapid kinetics with non-precious materials and produces high quality heat for energy conversion or other uses.
- The SOFC can appear in small-scale stationary applications.
- The SOFC is flexible to use many types of fuel, such as methane, methanol, ethanol, or gasoline.

Two types of solid electrolytes can be employed in the SOFC, i.e. oxygen ion-conducting and proton-conducting electrolytes. The difference between both electrolyte types is the location of the water produced. With the oxygen ion-conducting electrolyte (see Fig.2.7), water is produced in the reaction mixture in the

anode chamber. In the case of the proton-conducting electrolyte (see Fig. 2.8), water appears on the cathode side. The reactions taking place in the anode and the cathode can be summarized as follows:

- Oxygen ion-conducting electrolyte (SOFC- O^{2-}):



- Proton-conducting electrolyte (SOFC- H^+):

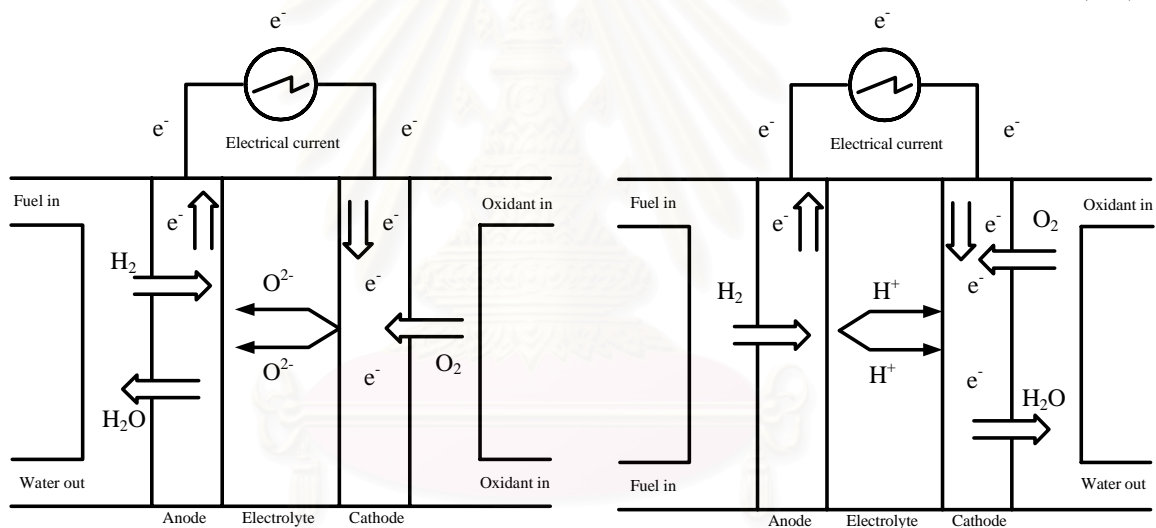
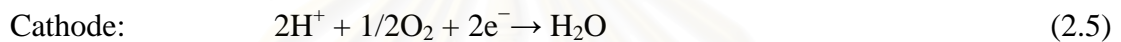


Fig. 2.7 Oxygen ion-conducting electrolyte **Fig. 2.8** Proton-conducting electrolyte

When SOFCs are operated with a fuel, such as hydrocarbon and alcohol, three modes of operation, i.e. external reforming SOFC (ER-SOFC), indirect internal reforming SOFC (IIR-SOFC) and direct internal reforming SOFC (DIR-SOFC) as shown in Fig. 2.9, are possible. For ER-SOFC operation, the endothermic steam reforming and the electrochemical reactions are operated separately in different units, and there is no direct heat transfer between both units. High energy supply to the outside reformer is required due to the high endothermic over this part. In contrast, for both IIR-SOFC and DIR-SOFC, the endothermic reaction from the steam reforming reaction and the exothermic reaction from the oxidation reaction are operated together

in a single unit. Therefore, the requirement of a separate fuel reformer and energy supply to this unit can be eliminated. This configuration is expected to simplify the overall system design, making SOFC more attractive and efficient means of producing electrical power. For IIR-SOFC, the reforming reaction occurs in the vicinity of the cell stack. This enables heat transfer from the fuel cell chamber to the reformer, which leads to energetic economy. However, part of heat may not be efficiently utilized due to its limited heat transfer rate. For DIR operation, the reforming reaction takes place at the anode of the fuel cell. Heat and steam released from the electrochemical reaction upon power generation is effectively used for the endothermic reforming reaction since both processes take place simultaneously at the anode. Therefore, in term of energy aspect, DIR-SOFC is more attractive than the others. It should be noted that state-of-the-art SOFC nickel cermet anodes can provide sufficient activity for the steam reforming and shift reactions without the need for additional catalysts (Clarke *et al.*, 1997; Dick 1998).

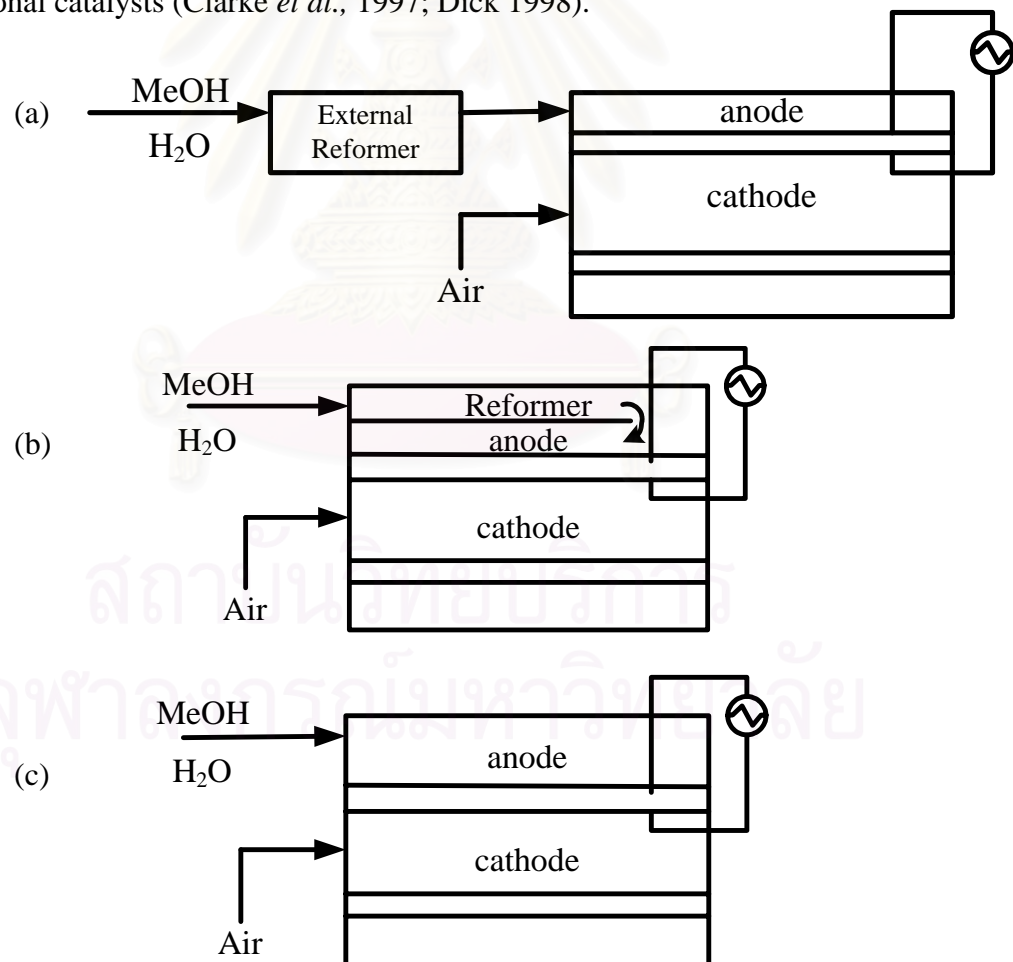


Fig. 2.9 Configurations of various SOFC modes (a) ER-SOFC, (b) IIR-SOFC and (c) DIR-SOFC

The electromotive force (E_o) of a cell is the difference in the potential of the two electrodes. Thus, the electromotive force can be represented as follows:

$$E_o = |\varphi_c - \varphi_a| \quad (2.6)$$

$$E_o = \frac{\Delta G}{n_e F} \quad (2.7)$$

where φ_c and φ_a are the potentials of the cathode and the anode respectively. The electrode potential can be calculated from Nernst equation.

The theoretical open-circuit voltage is the maximum voltage that can be achieved by a fuel cell under specific operating conditions. The operating voltage is less than the electromotive force because of overpotential. The losses are common to all types of fuel cells and cannot be eliminated, although temperature, pressure, gas flow rate and composition, electrode and electrolyte materials, and cell design, all influence their magnitude. The difference or the voltage drop was resulted from three major irreversibilities or losses.

$$V = E_o - (\eta_{ohm} + \eta_{Act,a} + \eta_{Act,c} + \eta_{Conc,a} + \eta_{Conc,c}) \quad (2.8)$$

where E_o is open circuit voltage determined by Eq. 2.7 and η_i is type of overpotential in each electrodes

Ohmic Overpotential (Ohm)

Ohmic overpotentials are caused by resistance to conduction of ions, (through the electrolyte) electrons, (through the electrode) current, and from contact resistance between cell components. This voltage drop is important in all types of cells and is essentially linear and proportional to current density.

Activation Overpotential (Act)

Activation overpotential is controlled by the electrode kinetics at the electrode surface. This polarization is directly related to the activation barrier that must be

overcome by the reacting species in order for the electrochemical reaction to occur. The electrode reaction rate at high temperatures is fast, leading to low activation polarization as commonly observed in SOFC.

Concentration Overpotential (Conc)

Concentration overpotential occurs when the fuel is consumed at the electrode–electrolyte interface, and the gas concentration decreases at the reaction sites. Concentration polarization becomes an important loss at high current densities and small fuel concentrations.

2.3 Solid Oxide Fuel Cell System

The simulation program is developed for SOFC system operated with methanol feed. This system as shown in Fig. 2.9 consists of pre-heaters, a SOFC stack, a reformer and an after burner. The reformer used is a steam reforming type.

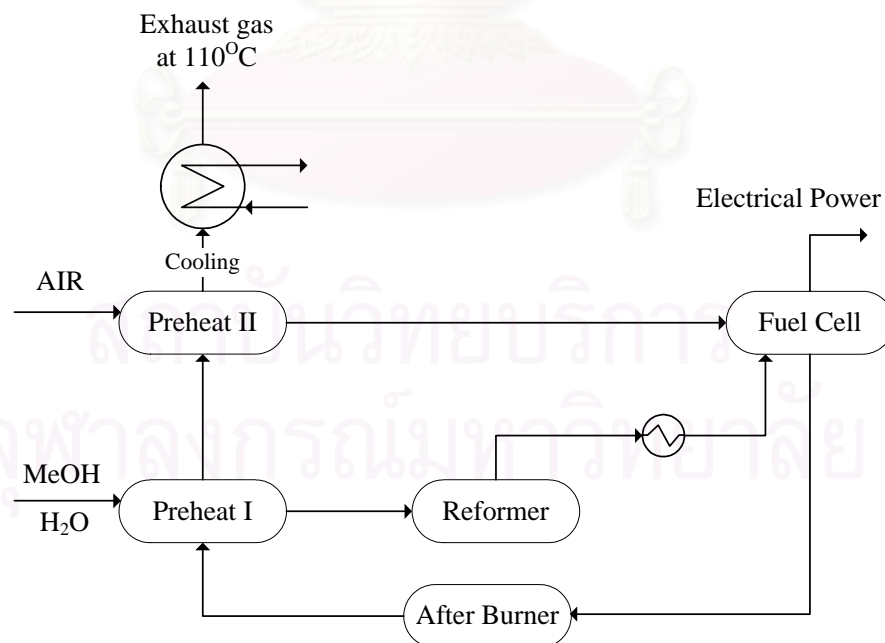


Fig.2.9 Solid Oxide Fuel Cell system

The assumptions and conditions of model used in the simulation program are listed as follows:

- ◆ Steady flow with negligible frictional losses.
- ◆ Negligible changes of potential and kinetic energies in any process.
- ◆ The environment is at STP condition, i.e. 298K and 1 atm.
- ◆ Isothermal processes in the fuel cell
- ◆ Adiabatic process in afterburner
- ◆ Default fuel supplying rate is 1 mol s^{-1} .
- ◆ Well diffusion at electrode so negligible concentration overpotential.

2.4 Palladium Membrane

Palladium was first identified as a highly hydrogen permeable material in the 19th century. Palladium purifiers provide <1 ppb purity with any inlet gas quality. Impurities removed include O₂, H₂O, CO, CO₂, N₂ and all hydrocarbons including methane (CH₄). Normal life expectancy of a palladium membrane purifier is 5 years and no routine maintenance required. Palladium has better than other material because of its catalysis surface.

Advantages of using palladium:

- Infinite hydrogen selectivity
- Temperature stability
- Corrosion resistance

The Mechanism of Hydrogen Diffusion

The mechanism of hydrogen diffusion involves a series of steps: (1) adsorption, (2) dissociation, (3) ionization, (4) diffusion, (5) recombination and (6) desorption. Several molecules of hydrogen and nitrogen atoms are on the metal surface. Within the metal, hydrogen loses its electron to the palladium structure and diffuses through the membrane as an ion (or proton). At the exit surface the reverse process occurs. Only hydrogen appears to possess the ability to diffuse through palladium or palladium alloys. Assuming no pinholes or micro-cracks, the hydrogen

issuing from the low-pressure side of a membrane may be looked upon as a standard of absolute purity. Attempts to detect the presence of impurities show only traces in the parts-per-billion range.

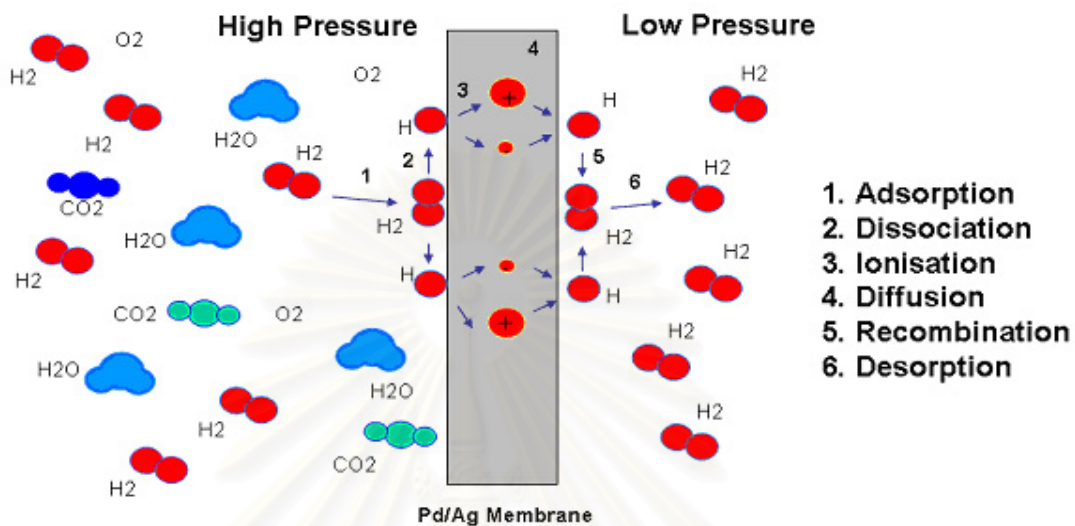


Fig. 2.10 Mechanism of Hydrogen diffusion in palladium membrane (From <http://www.matthey.com>)

สถาบันวิทยบริการ
จุฬาลงกรณ์มหาวิทยาลัย

CHAPTER III

LITERATURE REVIEWS

3.1 Fuel cell

Fuel cells continue to be the subject of extensive research and development. To provide the resources for R&D work, both public and private funds are being employed. Currently, the U.S. Department of Energy's Solid State Energy Convergence Alliance program (SECA) is funding the development of solid oxide fuel cell technology for both stationary power and auxiliary power applications (Williams *et al.*, 2005). The program is divided into three phases, and following each phase, testing is performed to ensure that progress is being made toward the goal of a viable commercial unit having power in the range of 3–10 kW and a cost less than \$400 kW⁻¹.

The fuel source can also affect cell lifetime. Sulfur compounds are contained in most commercial fuels. Matsuzaki and Yasuda (2000) showed that nickel anodes for SOFC's can be poisoned by such sulfur-gas to different amounts depending on time, temperature and impurity concentration. However, Aguilar *et al.* (2004) showed that degradation of SOFC's operated on sulfur containing fuels can be potentially improved with advances in new anode material.

3.2 Methanol steam reforming

The reactions involved in the production of hydrogen from the steam reforming of methanol can be represented by the widely accepted decomposition-shift mechanisms (Amphlett *et al.*, 1981).



Early studies (Amphlett *et al.*, 1988) showed that when in thermodynamic equilibrium the system contains only five species with noticeable concentration, namely: methanol, carbon monoxide, carbon dioxide, hydrogen and water. Recent work by Lwin *et al.* (2000) also confirmed that the equilibrium composition of other higher molecular weight compounds such as formaldehyde, methyl formate and formic acid are negligible. It was revealed, however, that methane formation according to Eq. (3.3) needed to be included in the calculation



Hydrogen for use in fuel cells is typically generated in a fuel processor from available fuels ($\text{C}_n\text{H}_m\text{O}_p$) by means of the reforming reaction. The reforming efficiency is correlated with the fuel properties to show that it depends on the values of “m” and “n”, and on the heat of formation of the feed. Ahmed *et al.* (2001) found that the steam reforming process yields the highest hydrogen concentration in the product.

Rostrup-Nielsen (2001) found that methanol reforming over Cu/Zn/Al catalyst mainly used for small hydrogen plants. The amount of heat required per mole of hydrogen is far less than steam reforming of natural gas and equipment becomes much cheaper.

3.3 Coke Formation

Although the steam reforming of methanol for hydrogen production is feasible from a thermodynamic point of view, a major consideration is carbon formation in the system. Appropriate operating conditions must be employed to avoid damage from carbon deposition such as catalyst deactivation in the reformer or anode deactivation in a SOFC with an internal reformer. The formation of carbon leads to loss of system performance and poor durability (Clarke *et al.*, 1997).

Coke formation is the major problem of steam reforming reaction. There have many methods to control this problem, for example: ensemble size control reduced by

adsorbing controlled amounts of sulfur on the nickel surface has been found to be very effective of controlling coking. Small amounts of tin reduce coking very significantly and the use of rare earth oxides as supports can also reduce coking (Trimm, 1999).

Addition of molybdenum and cerium metal oxides to the Ni-based anode was reported to reduce carbon deposition, and in some cases, to increase fuel conversion (Finnerty and Ormerod, 2000). The addition of alkalis such as potassium can accelerate the reaction of carbon with steam and also neutralize the acidity of the catalyst support, hence reducing carbon deposition (Finnerty *et al.*, 1998).

To avoid carbon formation, work at University of Pennsylvania, has focused on replacing Ni with catalytically inert Cu. Furthermore, the fabrication of Cu-based anodes has required the development of new synthetic methods, different from those used to produce Ni ceramic-metallic (cermet) composites, because CuO and Cu₂O melt at the temperatures required for processing YSZ (Gorte *et al.*, 2000).

Lwin *et al.* (2000) re-examined the steam reforming of methanol by the method of direct minimization of Gibbs free energy at temperatures in the range of 360 to 573 K and a H₂O: MeOH feed ratio of 0 to 1.5. It was found that the formation of carbon and methane was thermodynamically favoured and reduced both the quantity and the quality of the hydrogen produced. Undesired products such as dimethyl ether occurred at low temperatures and low H₂O: MeOH feed ratios.

For the steam reforming, addition of extra steam to the feed is a conventional approach to avoid carbon deposition. Selection of a suitable steam/hydrocarbon ratio becomes an important issue. Carbon formation can occur when the SOFC is operated at low steam/hydrocarbon ratio. However, use of high steam/hydrocarbon ratio is unattractive as it lowers the electrical efficiency of the SOFC by steam dilution of fuel and the system efficiency (Park, *et al.*, 2000).

In selection of suitable steam to fuel ratio can be an alternative for avoid in the coke formation problem. Methanol has the least steam to fuel ratio compared with ethanol, methane and gasoline (Douvartzides *et al.*, 2003(b)). For all cases, the

required steam per fuel ratio for avoiding coke formation is decreased when temperature operating is increased and the effect of hydrogen consumption depends on the types of electrolytes (Lwin *et al.*, 2000).

3.4 Fuel cell system analysis

The efficiency of SOFC system and electromotive force (EMF) are function of the amount of carbon atoms of the fuel as well as of the operating temperature. The steam to fuel ratio has been adjusted to be low enough so as to ensure optimal conditions in the SOFC operation but high enough to avoid carbon formation (Coutelieris *et al.*, 2003).

Mathematic modeling is an essential tool for the design of SOFC system. For intermediate temperature direct internal reforming (IT DIR-SOFC); cathode activation overpotentials represent the major sources of voltage loss for co-flow operated at steady state condition (Aguiar *et al.*, 2004). Comparison of steady state and dynamic models at same condition showed good agreement between both models in terms of the overall performance. However the discrepancies between the two models increase, especially in the fuel channel when higher current density values are assigned to the cell (Iora *et al.*, 2005). Considering a steady state model of IIR-SOFC (indirect internal solid oxide fuel cell), the results have shown that a local cooling of heat, undesirable for ceramic fuel cells, appears close to the reformer entrance. Increasing the operating pressure is shown to be an effective way of reducing both the local cooling (Aguiar *et al.*, 2002). For internal reformer, the operating conditions such as fuel recirculation, fuel inlet temperature, air circulation and air inlet temperature have considerable effects on the exhaust temperature but a slight effect on the efficiency (Nagata *et al.*, 2000). A simulation model for the Intergrated Planar Solid Oxide Fuel Cell (IT-SOFC) showed that activation overpotential is the major source of voltage drops and vary with current density and anode thickness but inverse to hydrogen molar fraction (Costamagna *et al.*, 2004)

Demin and Tsiakaras (2001) showed that efficiency of SOFC with hydrogen conducting (SOFC-H⁺) is higher than SOFC with oxygen conducting (SOFC-O²⁻). It was also estimated that SOFC-H⁺ efficiency at 1000 K is about 70% when it runs at

60% of its maximum power, whereas the practically reachable SOFC-O²⁻ efficiency under the above mentioned conditions is less than 55%. Then they used ethanol as fuel and found that efficiency of SOFC is about 20% less than the maximum SOFC system efficiency in the previous case. When temperature is increased, SOFC system efficiency is decreased (Tsiakaras and Demin, 2001). In some cases, ethanol can be operated at low temperature (933-1073 K) with complete oxidation (Galvia *et al.*, 2002). The products from that process at higher temperature (1073 K) facilitated synthesis gas production. Thermodynamic analysis of methane fed SOFC-H⁺ system is preformed. It was stated that the fuel utilization depends on H₂O/CH₄ mole ratio in the feeding fuel mixture and has a mixture at the ratio about 2.6 and maximum efficiency of SOFC-H⁺ system is about 15% higher than of SOFC system based on SOFC-O²⁻ (Demin *et al.*, 2002).

The special case of ion transport in the co-ionic electrolyte was analyzed. It was shown that partial ion current does not correspond to ion transfer numbers. It was established that the maximum achievable efficiency of a hydrogen-fed SOFC based on the co-ionic electrolyte with proton transfer number of 0.5, is 0.78 at 1173 whereas the efficiency is 0.62 when the SOFC works at 70% of its maximum power (Demin *et al.*, 2004).

System efficiencies can be considered into 2 types; i.e. energetic method (1st laws efficiency) and exergetic method (2nd laws efficiency). Both of them are considered for performance analysis. The results obtained from natural gas reforming thermodynamics simulation indicates that SOFC is more efficient than MCFC (Molten Carbonate Fuel Cell) and the carbon dioxide emission of SOFC is lower than MCFC one (Matelli and Bazzo, 2004). Energy conversion efficiency of ethanol into electricity was maximized considering a SOFC power plant with ethanol steam reforming, an after burner, a vaporizer and two heat exchangers based on mathematical model. The exergy analysis was applied to provide design criteria in terms of the temperature of the reforming and preheating (Douvartzides *et al.*, 2003(a)). In the same system, methane-fed SOFC presents higher 1st law efficiency and 2nd law efficiency than ethanol-fed SOFC (Douvartzides *et al.*, 2004; Bedringas *et al.*, 1997).

Braun, *et al.* (2005) considered combined heat and power (CHP) solid oxide fuel cell. The results indicated that maximum efficiency is achieved when cathode and anode gas recirculation is used along with internal reforming of methane. System electric efficiencies of 40% HHV (45% LHV) and combined heat and power efficiencies of 79% (88% LHV) are described. The amount of heat loss from small-scale SOFC systems is included in the analyses and can have an adverse impact on CHP efficiency. Performance comparisons of hydrogen-fueled versus methane-fueled SOFC systems are also given. The comparisons indicated that hydrogen-based SOFC systems do not offer efficiency performance advantages over methane-fueled SOFC systems.

3.5 Pd membrane

The hydrogen permeability of palladium increases with temperature because the endothermic activation energy for diffusion dominates the exothermic adsorption of hydrogen on palladium. Buxbaum, *et al.* (2002) found that conversion of methanol steam reforming in palladium membrane reactor decreased with increasing reforming pressure but percentage of hydrogen recovery was increased. If oxygen is added to the hydrogen supply upstream side, hydrogen permeation decreases due to the efficient catalytic formation of water on the surface of the palladium membrane. When adding oxygen on the other side, permeated hydrogen will react with oxygen to form water, lowering the hydrogen partial pressure on the downstream side close to zero and consequently the effective hydrogen permeation rate increases. (Amanduson *et al.*, 1999)

Latter *et al.* 2004 studied the benefit of Pd membrane in polymer exchange membrane (PEM) fuel cell system. They found that the main advantages of a palladium membrane reactor are (i) a reduction in the fuel processor volume, (ii) a small improvement in the overall system efficiency due to elimination of hydrogen losses in the PrOx step and (iii) the use of a steam sweep for the permeate provides a pre-humidified anode feed gas.

CHAPTER IV

DETERMINATION OF BOUNDARY OF CARBON FORMATION FOR SOFC WITH DIFFERENT ELECTROLYTE TYPE

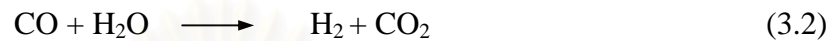
Summary

A detailed thermodynamic analysis is undertaken for carbon formation in a solid oxide fuel cell (SOFC) with a direct internal reformer (DIR) fuelled by methanol. Two types of fuel cell electrolyte, i.e. oxygen ion and proton-conducting, are considered. Equilibrium calculations are performed to find the range of inlet steam: methanol ($\text{H}_2\text{O}:\text{MeOH}$) ratio where carbon formation is thermodynamically unfavourable in the temperature range of 500 to 1200 K. The key parameters that determine the boundary of carbon formation are temperature, type of solid electrolyte, and the extent of the electrochemical reaction of hydrogen. The minimum $\text{H}_2\text{O}:\text{MeOH}$ ratio for which carbon formation is thermodynamically unfavoured decreases with increasing temperature. Comparison between the two types of electrolyte reveals that the proton-conducting electrolyte is not attractive for use in term of the tendency of carbon formation.

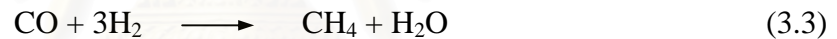
สถาบันวิทยบริการ
จุฬาลงกรณ์มหาวิทยาลัย

4.1 Calculation of the converted mole of methanol steam reforming

The methanol steam reforming to produce hydrogen can be represented by widely accepted decomposition-shift mechanisms (Amphlett *et al.*, 1981):



The methanol steam reforming reaction produces gas mixture in thermodynamic equilibrium. It contains only five components which are carbon monoxide, carbon dioxide, hydrogen, water and methane. Lwin *et al.* (2000) confirmed that the equilibrium compositions of other higher molecular weight compounds such as formaldehyde, methyl formate and formic acid are negligible. It was revealed, however, that methane formation according to Eq. (3.3) needed to be included in the calculation.



When the SOFC is operated with an internal reformer, part of the proton produced is consumed by the electrochemical reaction with oxygen producing water and electricity. Two types of solid electrolyte can be employed in SOFC operation, via, oxygen ion and proton-conducting electrolytes. An oxygen ion-conducting electrolyte is common for the use in SOFCs, while a proton-conducting electrolyte is normally used in low-temperature fuel cells (e.g., PEM and PAFC). It should be noted that some types of proton-conducting electrolyte are not classified as solid oxides and the term ‘ceramic fuel cell’ is more preferable in these cases. The difference between both types of electrolyte is the location at which the water is produced. With an oxygen ion-conducting electrolyte, water is produced in the reaction mixture in the anode chamber. By contrast, with a proton-conducting electrolyte, water appears on the cathode side. In this work, a SOFC with a proton-conducting electrolyte is studied as an alternative approach and is used for comparison purposes. The number of moles of each component is given by the following expressions:

$$n_{MeOH} = a - x_1$$

$$n_{CH_4} = x_3$$

$$n_{CO} = x_1 - x_2 - x_3$$

$$n_{CO_2} = x_2$$

$$n_{H_2} = 2x_1 + x_2 - 3x_3 - c \quad (\text{for SOFC-O}^{2-})$$

$$n_{H_2} = 2x_1 + x_2 - 3x_3 - c \quad (\text{for SOFC-H}^+)$$

$$n_{H_2O} = b + c - x_2 + x_3 \quad (\text{for SOFC-O}^{2-})$$

$$n_{H_2O} = b - x_2 + x_3 \quad (\text{for SOFC-H}^+)$$

$$n_{tot} = \sum_{i=1}^6 n_i$$

Hence $n_{tot} = a + b + 2x_1 - 2x_3 \quad (\text{for SOFC-O}^{2-})$

$$n_{tot} = a + b - c + 2x_1 - 2x_3 \quad (\text{for SOFC-H}^+)$$

where

n_i is mol of substance i

a is inlet mole of methanol

b is inlet mole of water

c is extent of the electrochemical reaction of hydrogen

x_i is the converted moles associated to the reactions (3.1) to (3.3),

respectively

The equilibrium constants (K) whose values can be determined from the change in Gibb's free energy of the reaction can be expressed as follows (more details are given in App. B):

$$K_1 = \frac{p_{H_2}^2 p_{CO}}{p_{MeOH}} \quad (4.1)$$

$$K_1 = \frac{\left(\frac{2x_1 + x_2 - 3x_3 - c}{a + b + 2x_1 - 2x_3}\right)^2 \left(\frac{x_1 - x_2 - x_3}{a + b + 2x_1 - 2x_3}\right)}{\left(\frac{a - x}{a + b + 2x_1 - 2x_3}\right)} \quad (4.2i)$$

$$K_1 = \frac{\left(\frac{2x_1 + x_2 - 3x_3 - c}{a + b + 2x_1 - 2x_3 - c}\right)^2 \left(\frac{x_1 - x_2 - x_3}{a + b + 2x_1 - 2x_3 - c}\right)}{\left(\frac{a - x}{a + b + 2x_1 - 2x_3 - c}\right)} \quad (4.2ii)$$

$$K_2 = \frac{P_{H_2} P_{CO_2}}{P_{CO} P_{H_2O}} \quad (4.3)$$

$$K_2 = \frac{\left(\frac{2x + x_2 - 3x_3 - c}{a + b + 2x_1 - 2x_3}\right) \left(\frac{x_2}{a + b + 2x_1 - 2x_3}\right)}{\left(\frac{x_1 - x_2 - x_3}{a + b + 2x_1 - 2x_3}\right) \left(\frac{b + c - x_2 - x_3}{a + b + 2x_1 - 2x_3}\right)} \quad (4.4i)$$

$$K_2 = \frac{\left(\frac{2x + x_2 - 3x_3 - c}{a + b + 2x_1 - 2x_3 - c}\right) \left(\frac{x_2}{a + b + 2x_1 - 2x_3 - c}\right)}{\left(\frac{x_1 - x_2 - x_3}{a + b + 2x_1 - 2x_3 - c}\right) \left(\frac{b + c - x_2 - x_3}{a + b + 2x_1 - 2x_3 - c}\right)} \quad (4.4ii)$$

$$K_3 = \frac{P_{CH_4} P_{H_2O}}{P_{CO} P_{H_2}^3} \quad (4.5)$$

$$K_3 = \frac{\left(\frac{x_3}{a + b + 2x_1 - 2x_3}\right) \left(\frac{b + c - x_2 - x_3}{a + b + 2x_1 - 2x_3}\right)}{\left(\frac{x_1 - x_2 - x_3}{a + b + 2x_1 - 2x_3}\right) \left(\frac{2x_1 + x_2 - 3x_3 - c}{a + b + 2x_1 - 2x_3}\right)^3} \quad (4.6i)$$

$$K_3 = \frac{\left(\frac{x_3}{a+b+2x_1-2x_3-c} \right) \left(\frac{b+c-x_2-x_3}{a+b+2x_1-2x_3-c} \right)}{\left(\frac{x_1-x_2-x_3}{a+b+2x_1-2x_3-c} \right) \left(\frac{2x_1+x_2-3x_3-c}{a+b+2x_1-2x_3-c} \right)^3} \quad (4.6ii)$$

where i and ii represented oxygen ion-conducting electrolyte and proton-conducting respectively.

System of non-linear equations was solved by developing a Matlab program using the Newton's method as a solving algorithm (See Appendix C).

4.2 Determining of boundary of carbon formation

The following four reactions are the most probable reactions that lead to carbon formation in reaction systems.



At low temperature, the reactions (Eqs. 4.9 and 4.10) are favourable while the reaction (4.8) is thermodynamically unfavoured. The Boudard reaction (Eq. 4.7) and the decomposition of methane (Eq. 4.8) are the major pathways for carbon formation at high temperature as they show the largest change in Gibbs energy. It should be noted that due to the exothermic nature of the water-gas shift reaction and the methanation reaction amount of CO becomes significant at high temperature (Brown *et.al.*, 2001). The reactions give by Eqs. (4.7) and (4.8) are employed to examine the thermodynamic possibility of carbon formation. The carbon activities, defined in Eqs. (4.11) to (4.14), are used to determine the possibility of carbon formation.

$$\alpha_{c_1} = K_{c_1} \frac{P_{CO}^2}{P_{CO_2}} \quad (4.11)$$

$$\alpha_{C_2} = K_{C_2} \frac{P_{CH_4}}{P_{H_2}^2} \quad (4.12)$$

$$\alpha_{C_3} = K_{C_3} \frac{P_{CO} P_{H_2}}{P_{H_2O}} \quad (4.13)$$

$$\alpha_{C_4} = K_{C_4} \frac{P_{CO_2} P_{H_2}^2}{P_{H_2O}^2} \quad (4.14)$$

Where K_i is the equilibrium constant of the reaction (4.7) to (4.10) respectively

p_i is the partial pressure of component i

When $\alpha_C > 1$, the system is not in equilibrium and carbon formation is observed. The system is at equilibrium when $\alpha_C = 1$. Finally when $\alpha_C < 1$ carbon formation is thermodynamically impossible. It is noted that the amount of carbon in the system cannot be directly interpreted from the carbon activities. The latter are employed only as indicators of carbon formation. To find the range of SOFC operation that does not suffer from the formation of carbon, the operating temperature and the extent of the electrochemical reaction of hydrogen are specified. Then, the initial value of the water per methanol ratio is varied and the corresponding value of α_C is calculated. “The boundary of carbon formation” is defined as the water per methanol ratio that has a value of $(1-\alpha_C)$ close to zero. This value represents the minimum water per methanol ratio in the initial system at which carbon formation in the equilibrium mixture is thermodynamically impossible. It should be noted that other factors such as mass and heat transfer or the rate of reactions may also affect the prediction of the carbon formation boundary. Local compositions that allow carbon formation may exist, although such formation is unfavourable according to the calculation based on the equilibrium bulk compositions. In addition, it should be noted that although recent investigators estimated the carbon concentration in steam reforming reactions by the method of Gibbs energy minimization, the simple principle of equilibrated gas to predict carbon formation used in this study is still meaningful. This is because the calculation is carried out to find the boundary of carbon formation where the carbon just begins to form

4.3 Results and Discussion

4.3.1 Effect of the extent of hydrogen consumption on anode components

In the DIR operation, hydrogen produced from the reforming reactions electrochemically reacts with oxygen ion from supplied air, resulting in steam. This reaction is an important element in electricity production from fuel cell. In this section, the effects of the extent of hydrogen consumption via this electrochemical reaction, c , on each component at the anode are discussed. Figs. 4.1 and 4.2 show the results for the fuel cell with the oxygen ion- and proton-conducting electrolytes, respectively.

For all operating conditions investigated, number of mole of methanol is close to zero. This is the result from the strong endothermic decomposition reaction (Eq. 3.1) which is favored at high operating temperature of the SOFCs. For other species, it can be seen from Figs. 4.1 and 4.2 that the consumption of hydrogen by the electrochemical reaction affects their equilibrium concentrations. Constant removal of H_2 from the system via the electrochemical reaction shifts the equilibrium reactions of Eqs. 3.1 and Eq. 3.2 in forward direction while Eq. 3.3 in backward direction. Therefore, the carbon dioxide concentration increases whereas the carbon monoxide and methane concentrations decrease with an increase in the amount of hydrogen consumed. It should be noted that the changes in concentrations of those species with the amount of hydrogen consumed for the proton-conducting electrolyte system are less pronounced than those for the oxygen ion-conducting electrolyte system. The main difference between the uses of the oxygen ion- and proton-conducting electrolytes in SOFCs is the location where the electrochemical reaction mentioned above takes place. For the oxygen ion-conducting electrolyte system, that reaction occurs at the anode side. Therefore, the partial pressure of steam, which is the main product from the reaction, at the anode increases with higher extent of hydrogen consumption, as shown in Fig. 4.1. On the other hand, by using the proton-conducting electrolyte, steam is generated at the cathode side. The amount of steam in the anode slightly decreases with the higher extent of hydrogen consumption, as shown in Fig. 4.2, because the disappearance of hydrogen in the anode shifts the reactions that consume steam forward.

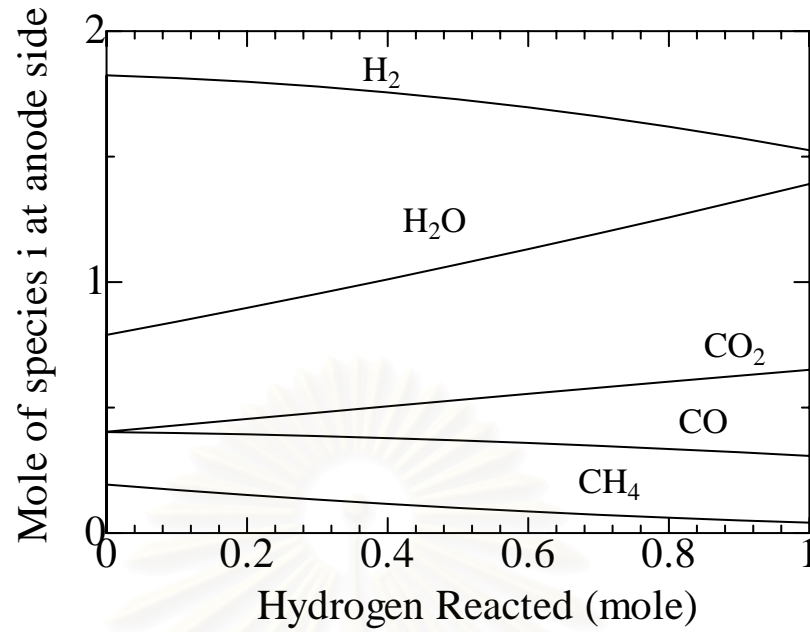


Fig. 4.1 Influence of the extent of the electrochemical reaction of hydrogen on moles of components at the anode side (oxygen ion-conducting electrolyte, $a = 1$ mol, $b = 1$ mol, $P = 1$ atm and $T = 1173$ K)

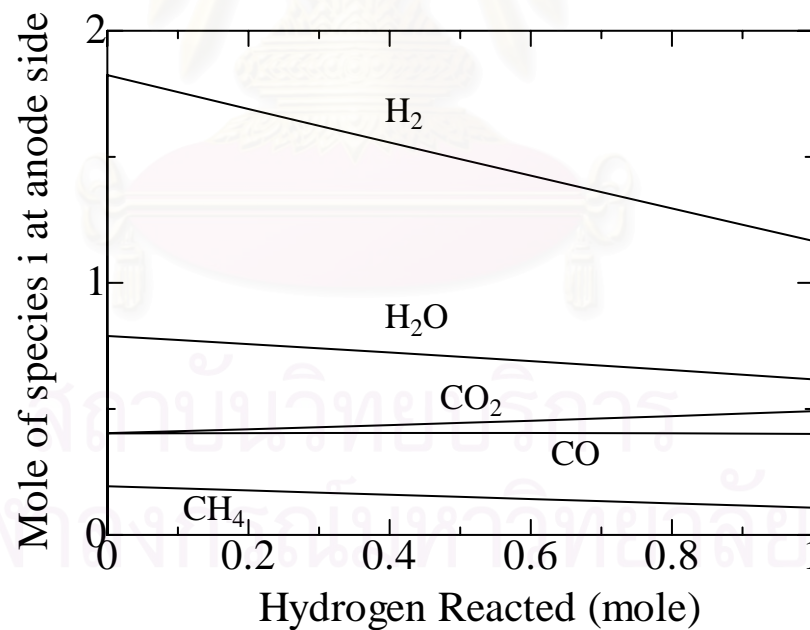


Fig. 4.2 Influence of the extent of the electrochemical reaction of hydrogen on moles of components in the anode side (proton-conducting electrolyte, $a = 1$ mol, $b = 1$ mol, $P = 1$ atm and $T = 1173$ K)

4.3.2 Effect of hydrogen consumption on carbon formation

Theoretically, the excess inlet steam reacts with carbon monoxide to form carbon dioxide according to the water-gas shift reaction (Eq. 3.2) and, in addition, helps preventing the formation of methane (Eq. 3.3). The increase in carbon dioxide concentration and the decrease in methane concentration subsequently prevent the possible carbon formation by the Boudard reaction (Eq. 4.7) and by the decomposition of methane (Eq. 4.8), respectively. Therefore, the formation of carbon is less likely in the oxygen ion-conducting electrolyte system because of the extra steam generated from the electrochemical reaction between hydrogen and oxygen ions at the anode side. Figs. 4.3(a) and 4.3(b) show the amount of each species in the anode side when the oxygen ion-conducting electrolyte is employed with $c = 0$ and 1.5 mol, respectively. It is evident, especially for the case of $c = 0$, that more carbon monoxide is converted to carbon dioxide when greater amount of steam is supplied to the system. Moreover, higher concentration of carbon dioxide is observed when the extent of the hydrogen consumption (c) is increased. The extra steam produced from the electrochemical reaction between hydrogen and oxygen ions enhances the water-gas shift reaction and retards the methanation reaction. Therefore, increasing the inlet H₂O: MeOH ratio in such system (i.e. when $c = 1.5$) decreases the amount of carbon monoxide and methane in the system.

The boundary of carbon formation, the minimum inlet H₂O: MeOH ratio at which the formation of carbon is thermodynamically unfavored, is represented in Figs. 4.4 and 4.5. The lines in the plots indicate the system in which carbon is in equilibrium with other species. In the region above the equilibrium line, carbon formation is thermodynamically impossible. Generally, the higher the temperature, the lower the boundary of carbon formation has found. This is the result from the decreasing of α_{c_1} , at high operating temperature, as the Boudard reaction (Eq. 4.7) is exothermic, and, in addition, the methane concentration at high temperature is small because of the strong exothermic methanation reaction. Therefore, increasing the SOFC operating temperature is one possibility to prevent carbon formation at the anode; however, the cost of high temperature materials and the problem of cell sealing must also be considered.

For the oxygen ion-conducting electrolyte system, the higher extent of hydrogen consumption (increasing of c) results in a decrease of the carbon formation boundary, as shown in Fig. 4.4. This is the result from the presence of extra steam from the electrochemical reaction as discussed earlier. It can be seen that the extent of this electrochemical reaction significantly affects the boundary of carbon formation. By using the same inlet H_2O : MeOH ratio, the system can be operated, without carbon formation, at remarkably lower temperature when the extent of hydrogen consumption is slightly increased. In the other words, the possibility of carbon formation on the anode of the SOFCs with the oxygen ion-conducting electrolyte is dramatically decreased if the electrochemical reaction between the generated hydrogen and supplied oxygen is maintained.

On the other hand, for the proton-conducting electrolyte system, a higher inlet H_2O : MeOH ratio is required to prevent possible carbon formation, as shown in Fig. 4.5. Higher amount of carbon monoxide and methane resides in the system while less carbon dioxide is produced from the water-gas shift reaction when the proton-conducting electrolyte is used, as shown earlier in Fig. 4.2. For the proton-conducting electrolyte, an increase in the extent of the electrochemical reaction of hydrogen (c) significantly demands higher inlet H_2O : MeOH ratio required to prevent carbon formation, especially at low operating temperature. This effect diminishes when the operating temperature is higher than 1173 K. Nevertheless, it is obvious that the oxygen ion-conducting electrolyte is more preferable due to the lesser tendency for carbon formation.

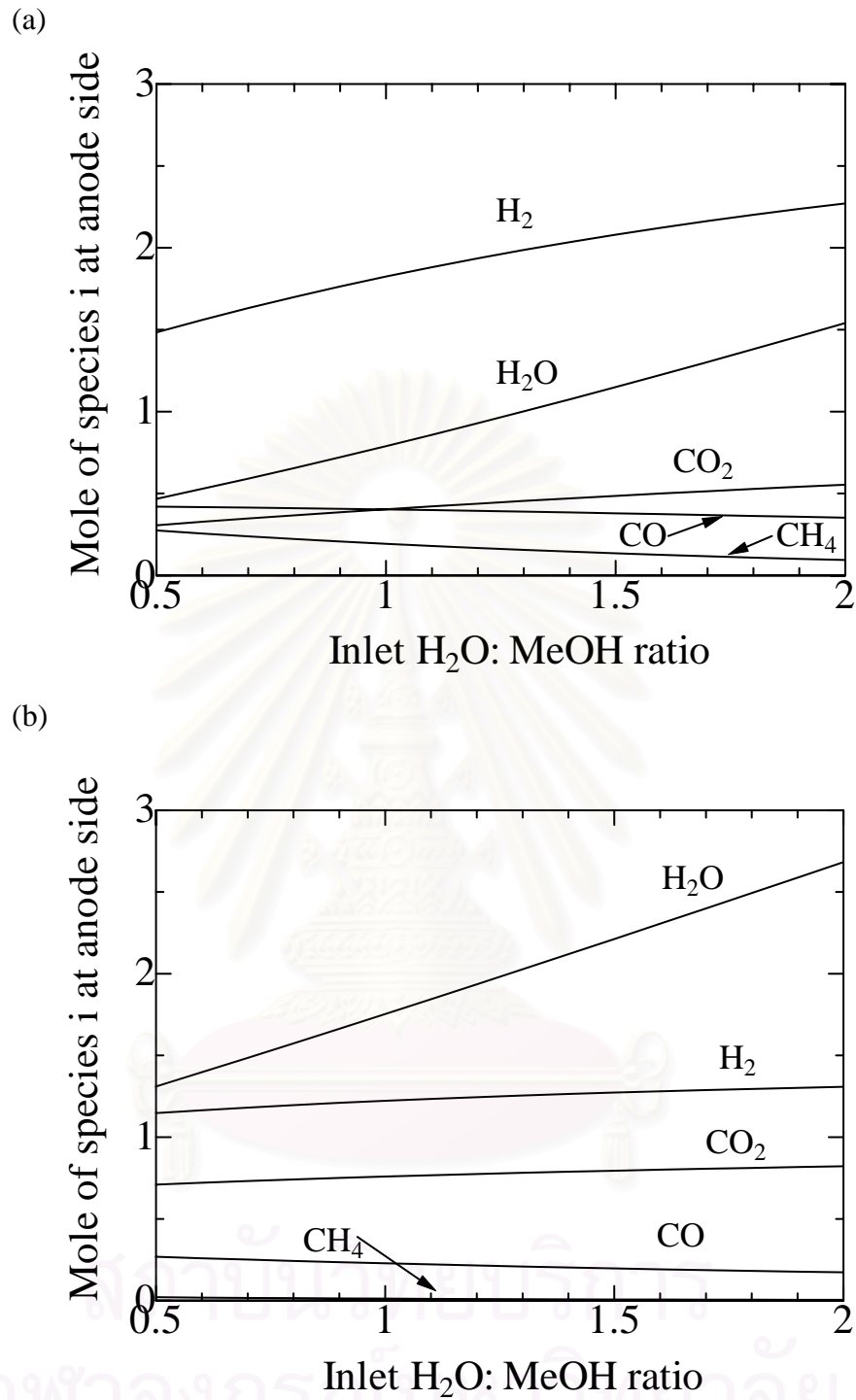


Fig. 4.3 Effect of inlet H_2O : MeOH ratio on each component mole at the anode side (oxygen ion-conducting electrolyte, $a = 1$ mol, $P = 1$ atm, $T = 1173$ K): (a) $c = 0$ mol, and (b) $c = 1.5$ mol

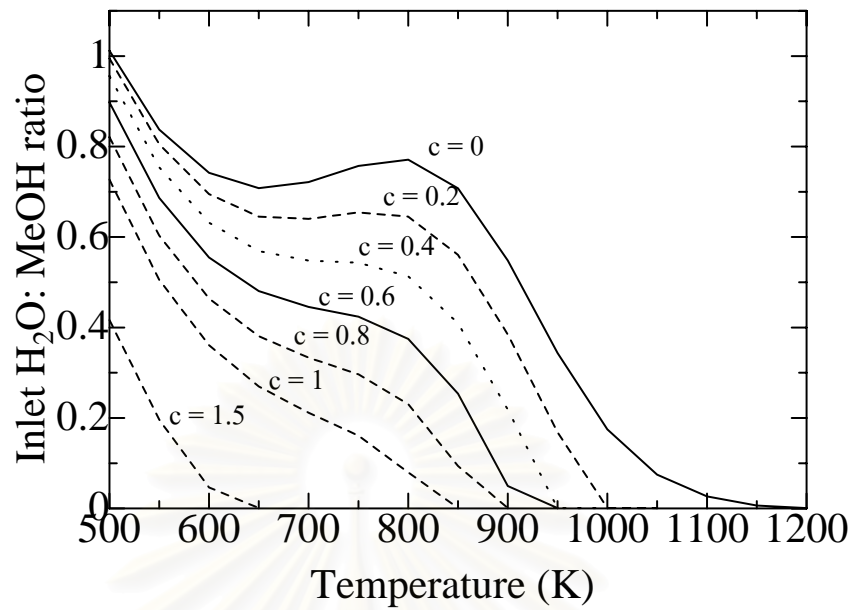


Fig. 4.4 Influence of the extent of the electrochemical reaction of hydrogen on the requirement of inlet H₂O: MeOH ratio at different operating temperatures (oxygen ion-conducting electrolyte, $a = 1$ mol, $P = 1$ atm)

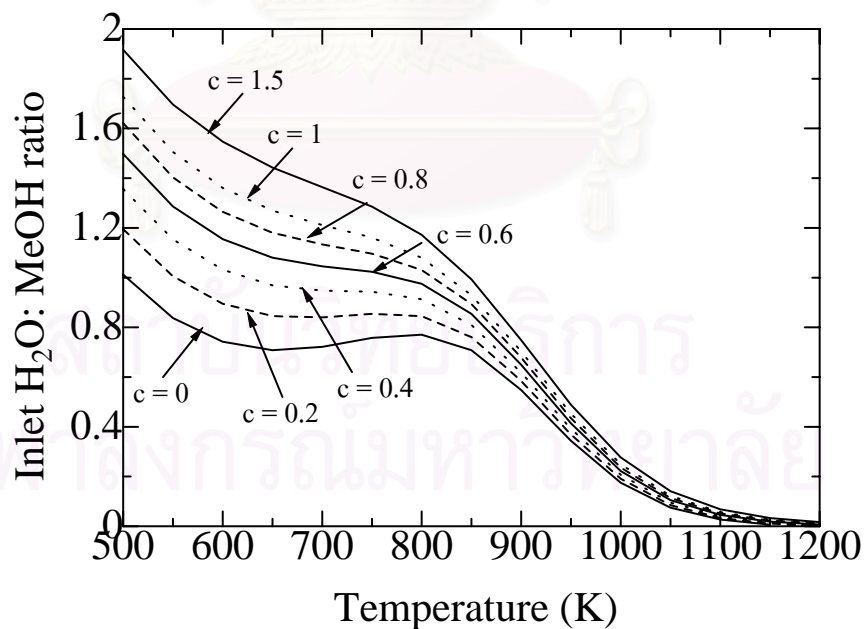


Fig. 4.5 Influence of the extent of the electrochemical reaction of hydrogen on the requirement of inlet H₂O: MeOH ratio at different operating temperatures (proton-conducting electrolyte, $a = 1$ mol, $P = 1$ atm)

The great benefit of the internal reforming operation is the coupling of the endothermic reforming reaction and the exothermic electrochemical reaction in a single unit. This coupling process is called an autothermal operation, which provides a thermal efficient approach for heat integration in SOFC. Another advantage of the DIR operation is reduction of the inlet steam requirement, as extra steam is supplied from the anode electrochemical reaction. The DIR operation must be carefully controlled during the start-up period, since the steam generated from the electrochemical reaction is expected to be less. Another advantage of using methanol as the fuel is reduction of the high-operating temperature requirement, because this component is easily reformed at low temperature. As described above, although direct internal reforming is expected to simplify the overall system design, this operation is not easy to achieve due to local mismatch between the rates of the endothermic and the exothermic reactions. This can lead to a significant reduction in the local temperature close to the entrance of the anode, which can result in possible carbon formation and also in mechanical failure due to thermally induced stresses. Therefore, this difficulty must also be considered as well as the mass transfer and heat transfer problems when using DIR in a SOFC. The impact of a SOFC-DIR with a proton-conducting electrolyte is comparable with membrane reactor operation in which hydrogen is removed from the system. Consequently, without careful control, carbon formation can be easily formed and result in possible catalyst or system damage. A higher inlet steam: carbon ratio could reduce this problem, but the additional energy requirement for water evaporation must then be considered.

4.4 Conclusions

A theoretical thermodynamic analysis has been performed to predict the boundary of carbon formation for a SOFC with direct internal reforming when methanol was used as fuel. The results indicate that carbon formation can be prevented by either increasing the inlet H_2O : MeOH ratio or by increasing the operating temperature. A comparison between the proton- and the oxygen ion-conducting electrolyte system shows that carbon formation in the latter system is less likely due to the extra steam that is produced from the electrochemical reaction of hydrogen at the anode.

CHAPTER V

THEORETICAL PERFORMANCE ANALYSIS OF SOFC WITH DIFFERENT ELECTROLYTE TYPE

Summary

Performances of methanol-fuelled solid oxide fuel cells (SOFCs) with different types of electrolyte (i.e., oxygen ion- and proton-conducting electrolytes) and flow patterns (i.e., plug flow (PF) and mixed flow (MF)) were investigated. Although it was demonstrated earlier that, under the same inlet steam: methane ratio, an SOFC with a proton-conducting electrolyte (SOFC-H⁺) thermodynamically offers higher efficiency than one with an oxygen ion-conducting electrolyte (SOFC-O²⁻), the benefit of a lower steam requirement for the SOFC-O²⁻ was not taken into account. Therefore, this study attempts to consider the benefit of differences in the steam requirement on the performance of SOFCs operated with different electrolytes and flow patterns. The efficiencies under the best conditions are compared in the temperature range of 900–1300 K. It is found that the maximum efficiencies decrease with increasing temperature and follow the sequence: SOFC-H⁺ (PF) > SOFC-O²⁻ (PF) > SOFC-H⁺ (MF) > SOFC-O²⁻ (MF). The corresponding inlet H₂O: MeOH ratios are at the carbon formation boundary for the SOFC-O²⁻ electrolyte, but are about 1.3–1.5 times the stoichiometric ratio for the SOFC-H⁺. It is clearly demonstrated that the PF mode is superior to the MF mode and that, although the benefit from the lower steam requirement is realized for the SOFC-O²⁻, the use of the proton-conducting electrolyte in the SOFCs is more promising.

5.1 Electrochemical reaction

In simple concept of fuel cell, electrochemical reaction is based on the simple combustion of hydrogen given by Eq. 5.1.



An electrochemical reaction is a reaction involving the transfer of charge as a part of a chemical reaction. The mechanism of this reaction is depended on electrolyte types. Two types of solid electrolytes can be employed in the SOFC, i.e. oxygen ion- and proton-conducting electrolytes. The reactions taking place in the anode and the cathode can be summarized as given earlier in Chapter 2. The difference between both electrolyte types is the location of the water produced. With the oxygen ion-conducting electrolyte, water is produced in the reaction mixture in the anode chamber. In the case of the proton-conducting electrolyte, water appears on the cathode side.

5.2 Theoretical performance

The electromotive force (E_0) of a cell is the difference in the potential of the two electrodes. Thus, the electromotive force can be represented as follows:

$$E_o = |\varphi_c - \varphi_a| \quad (5.2)$$

$$E_0 = \frac{\Delta G}{n_{\text{H}_2} F} \quad (5.3)$$

Where φ_c and φ_a are the potentials of the cathode and the anode respectively, the electrode potential can be calculated from Nernst equation (Eq.5.3). Because the electrochemical reactions at the electrodes are different, depending on the electrolyte type, the potential can be expressed as follows:

- Oxygen ion-conducting electrolyte:

$$\varphi = \frac{RT}{4F} \ln p_{r,O_2} \quad (5.4)$$

- Proton-conducting electrolyte:

$$\varphi = \frac{RT}{2F} \ln p_{r,H_2} \quad (5.5)$$

Where $p_{r,i}$ is the relative partial pressure of component i ($\frac{P_{c,i}}{P_{a,i}}$)

R is the universal gas constant

T is absolute temperature

F is Faraday constant

For SOFC-O²⁻, the partial pressure of oxygen in the cathode chamber is calculated from its mole fraction, while the following equation is used to determine the partial pressure of oxygen in the anode chamber.

$$P_{O_2} = \frac{P_{H_2O}}{K P_{H_2}^2} \quad (5.6)$$

For the SOFC-H⁺, the partial pressure of hydrogen in the anode chamber is calculated from its mole fraction, while the partial pressure of hydrogen in the cathode is given by:

$$P_{H_2} = \frac{P_{H_2O}}{K P_{O_2}^{1/2}} \quad (5.7)$$

In Eqs. (5.6) and (5.7), K is the equilibrium constant of the hydrogen oxidation reaction. Regarding the possible SOFC configurations, gas flow within the flow channels of the SOFC stack can be classified broadly into two ideal flow patterns, i.e., plug flow (PF) and mixed flow (MF). The former is characterized by the fact that the gas mixture moves orderly through the channel with no element of the gas mixing

with any other element ahead or behind, whereas with mixed flow the contents are well-mixed and uniform throughout. Although most typical SOFC are operated under a condition close to the PF mode, the MF mode can be realized by using a high recycle rate. In the PF mode, the electromotive force (E_0) changes along the SOFC stack due to the distribution of gas compositions along the flow channels in both the anode and the cathode sections.

The average electromotive force (\bar{E}) can be obtained from numerical integration of the gas distribution along the stack. To simplify the calculation, the gas compositions at the anode are assumed to reach their equilibrium compositions along the stack. The calculation procedures of the equilibrium compositions in SOFC have been described in previous chapter.

When current is drawn from the SOFC cell, the maximum electrical work (W) produced by the SOFC and the SOFC efficiency (Eff) defined as the ratio of the maximum conversion of the chemical energy of the fuel fed in the SOFC system to electrical work, are calculated from Eqs.(5.8) and (5.9), respectively.

$$W = q \bar{E} \quad (5.8)$$

$$Eff = \frac{q \bar{E}}{-\Delta H^0} \times 100\% \quad (5.9)$$

Where q is the electrical charge passing through the electrolyte and $-\Delta H^0$ is the lower heating value (LHV) of methanol at the standard condition.

It should be noted that the assumption of the equilibrium state of gas compositions along the flow channel may be reasonable because the rates of methanol steam-reforming and the water gas shift reaction are fast, particularly at high temperature and the conversion of methanol from the methanol steam-reforming always close to 100 % when the operating temperature above 573K is applied (Wild and Verhaak, 2000).

Moreover, at 1173 K, methanol steam-reforming has been reported to occur homogeneously and reach equilibrium. Deviation from this equilibrium condition would result in lower values of the electromotive force and the efficiency of SOFCs as less hydrogen would be generated in the anode chamber to compensate for the hydrogen consumed by the electrochemical reaction.

5.3 Results and Discussion

5.3.1 Effect of fuel utilization on theoretical performance

The efficiency and electromotive force at different fuel utilizations for methanol-fuelled SOFCs with different electrolyte types and flow patterns are shown in Fig. 5.1. The inlet steam: methanol ($\text{H}_2\text{O}:\text{MeOH}$) ratio is at the stoichiometric value of 1 for all SOFCs. The fuel utilization, U_f , is defined as the moles of hydrogen consumed by the electrochemical reaction divided by the maximum moles of hydrogen produced from the methanol steam-reforming (3 mol of hydrogen per 1 mol of methanol). As can be seen from Fig. 5.1(a), efficiencies increase with increasing fuel utilization for all SOFCs because more hydrogen is utilized for electrical power production. At high fuel utilization, however, the efficiencies of the SOFCs with the MF mode decrease, which corresponds to a sharp drop in the electromotive force observed in the MF mode (Fig. 5.1(b)). Although it is typical that the electromotive force decreases with increasing fuel utilization as the hydrogen partial pressure becomes smaller at higher fuel utilization, the flow characteristics of the PF mode allow the electromotive force to decrease gradually along the flow channel. Consequently, the PF mode provides a higher average electromotive force than the MF mode in which the electromotive force is at its minimum value over the entire cell area. It should be noted that although both ideal flow modes are not achieved in real operations, experimental SOFC using tubular and planar cells show behavior close to the PF and MF modes, respectively.

The results in Fig. 5.1 also show that the SOFC- H^+ offers higher efficiency than the SOFC- O^{2-} for both flow pattern modes. This is in good agreement with previous results obtained for SOFCs fuelled by hydrogen (Demin, *et al.*, 2001) and methane (Demin, *et al.*, 2002). The electrolyte type plays an important role on the

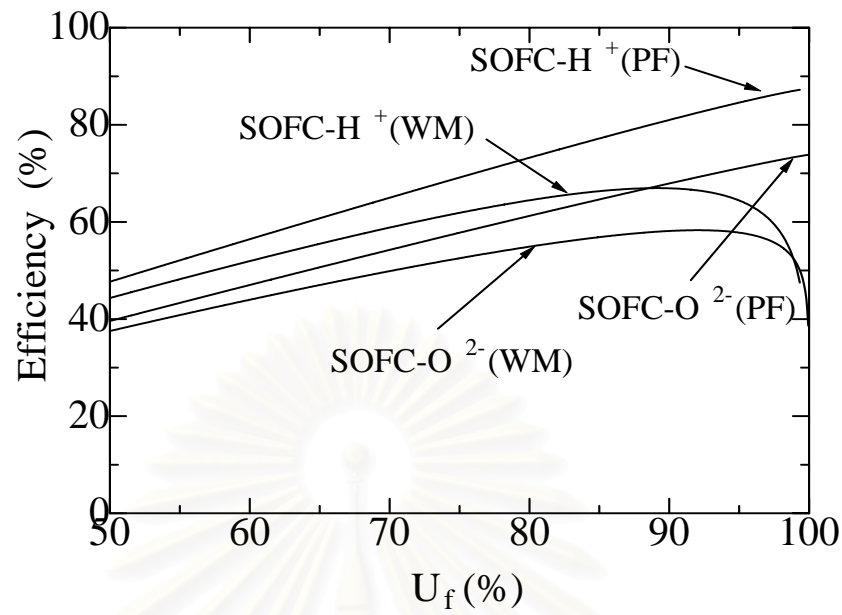
value of the hydrogen partial pressure in the anode side and, therefore, on the electromotive force and efficiency of the SOFC. The partial pressure of hydrogen for the SOFC-H⁺ is relatively higher than that for the SOFC-O²⁻ because the water generated from the electrochemical reaction is present and acts as an inert gas at the anode side for the SOFC-O²⁻, whereas it appears at the cathode side for the SOFC-H⁺. It is noted that when pure hydrogen is fed to the anode, the mole fraction of hydrogen in the anode chamber is always unity along the cell length for the SOFC-H⁺.

According to the above analysis for SOFCs with different electrolyte types and flow patterns under the same inlet H₂O: MeOH ratio, is demonstrated that the SOFC with the proton-conducting electrolyte operated under the PF mode (SOFC-H⁺ (PF)) is the most favorable choice.



สถาบันวิทยบริการ
จุฬาลงกรณ์มหาวิทยาลัย

(a)



(b)

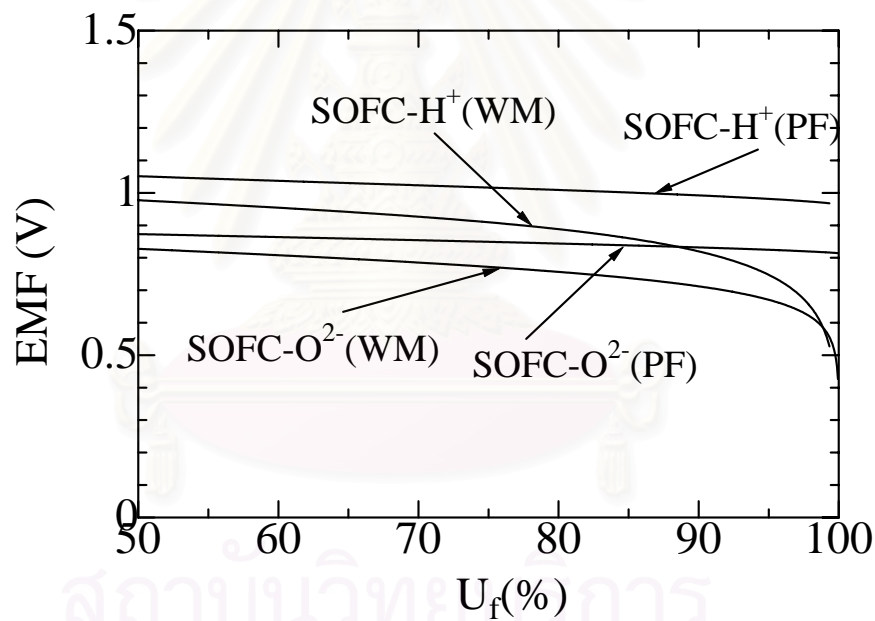


Fig.5.1 Performance of SOFC-O²⁻ and SOFC-H⁺ operated under plug flow (PF) and mixed flow (MF): (a) efficiency; (b) electromotive force (inlet H₂O: MeOH = 1, $T = 1173$ K, $P = 1$ atm)

5.3.2 Effect of inlet mole ratio on theoretical performance

In previous chapter it was shown that the steam requirement to operate the SOFC without carbon formation for the SOFC-O²⁻ is lower than that of the SOFC-H⁺. Thus, it is important to take into account this benefit in efficiency comparisons between different SOFCs. The effect of the inlet H₂O: MeOH ratio on the efficiency and electromotive force of the SOFC at the fuel utilizations of 90 % (solid lines) and 99 % (dashed lines) is presented in Fig. 5.2. The minimum inlet H₂O: MeOH ratios represent values at the carbon formation boundary. Details of the calculations for the carbon formation boundary in each operating mode have been described in the previous chapter. It was found that the SOFC-O²⁻ can be operated at the carbon-free condition without a requirement for extra steam in the methanol feed, and both the efficiency and electromotive force decrease with an increase in the inlet H₂O: MeOH ratio. Therefore, an addition of steam in the feed lowers the performance of the SOFC-O²⁻. For the SOFC-H⁺, the inlet H₂O: MeOH ratios at the carbon formation boundary are higher than those for the SOFC-O²⁻, particularly at high fuel utilization, and the effect of the inlet H₂O: MeOH ratio on the SOFC performance is less pronounced. As the water from the electrochemical reaction is generated at the cathode side, additional steam is required in the methanol feed at the anode side to promote hydrogen production. On the other hand, excessive steam will reduce the hydrogen concentration of the gas mixture at the anode side.

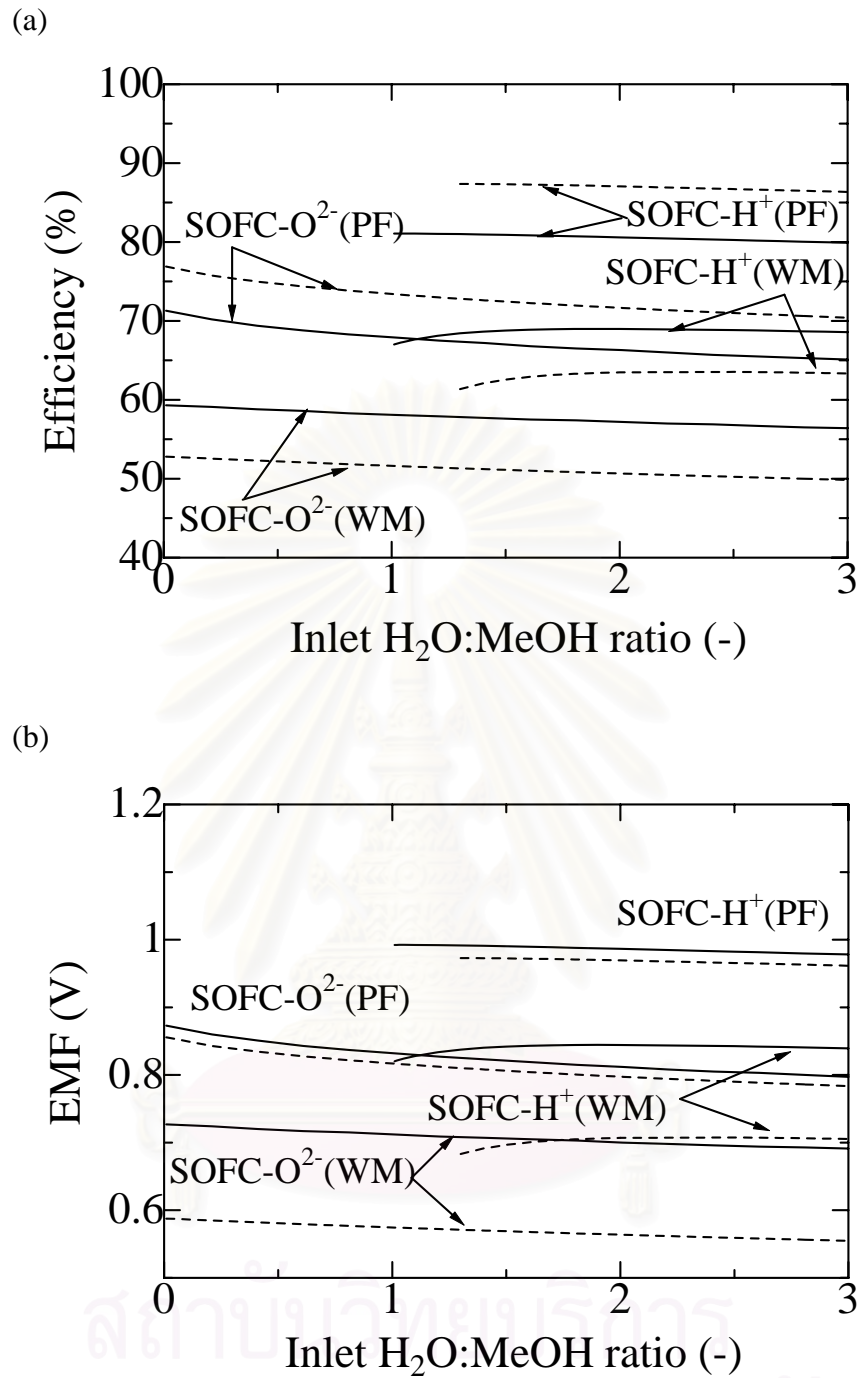


Fig. 5.2 Influence of inlet H₂O: MeOH ratio on SOFC performance at fuel utilization of 90 % (solid line) and 99 % (dashed line): (a) efficiency; (b) electromotive force ($T = 1173 \text{ K}$, $P = 1 \text{ atm}$)

5.3.3 Maximum efficiency

As it has been found that the SOFC performance is dependent on fuel utilization and inlet H₂O: MeOH ratio, it is possible to determine the maximum efficiency and the corresponding conditions for all SOFC cases at a specified temperature by performing calculations at various values of the inlet H₂O: MeOH ratio and the fuel utilization. The results for a temperature range of 900–1300 K are shown in Figs. 5.3 and 5.4.

The maximum efficiency for all cases decreases with increasing temperature. This is in good agreement with the decrease in electromotive force due to the thermodynamic Gibb's free energy.

The maximum efficiencies follow the sequence: SOFC-H⁺ (PF) > SOFC-O²⁻ (PF) > SOFC-H⁺ (MF) > SOFC-O²⁻ (MF). The corresponding inlet H₂O: MeOH ratios are at the carbon formation boundary for both the SOFC-O²⁻ (PF) and SOFC-O²⁻ (MF), but are about 1.3 and 1.5 times the stoichiometric ratio for the SOFC-H⁺ (MF) and the SOFC-H⁺ (PF), respectively. The values of fuel utilization at the maximum efficiency are mainly governed by the flow pattern. For SOFCs operated under the PF mode, the utilization is constant at approximately 99 %, but decreases slightly from 96.1 to 92.3 % and from 95.5 to 92.0 % for the SOFC-H⁺ (MF) and the SOFC-O²⁻ (MF), respectively, when the temperature is increased from 900 to 1300 K. From these results, it is obvious that the proton-conducting electrolyte is more preferable for use in SOFC. In addition, the PF mode is better than the MF mode. The SOFC-H⁺ provides approximately 7.7–10.6 % higher efficiency than the SOFC-O²⁻ with the same flow pattern mode in the range of temperature studied.

From the above studies, it is found that although the benefit of lower steam requirement is taken into account in the calculations for the SOFC-O²⁻, the SOFC-H⁺ still shows higher efficiency than the SOFC-O²⁻ for both the PF and the MF modes. This implies that the development of SOFCs should be directed towards the use of the proton-conducting electrolyte. It should also be noted, however, that this study has not taken into account all the losses presented in real SOFC operation and, therefore, it should be further investigated by taking into account these losses.

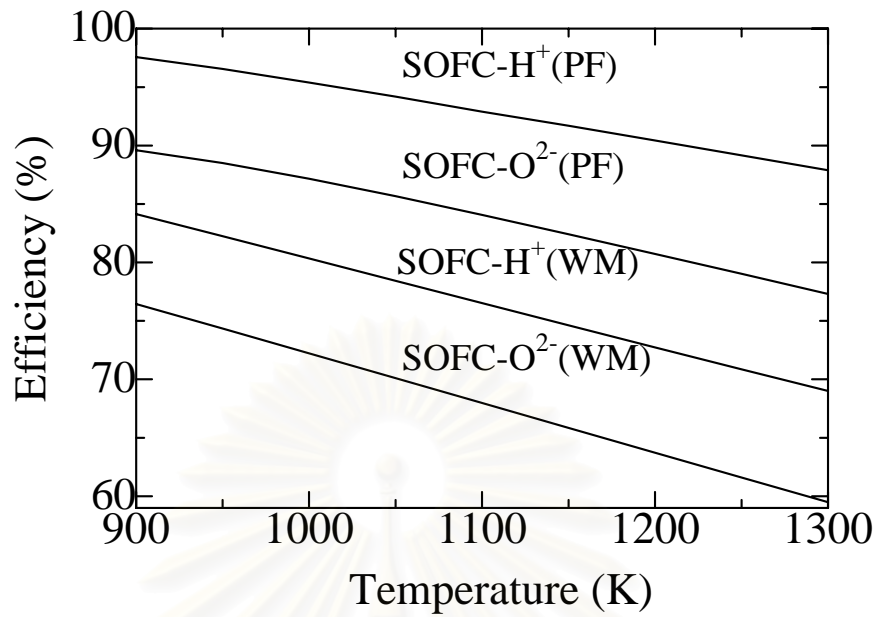


Fig.5.3. Maximum efficiency of different SOFCs at different operating temperatures ($P = 1 \text{ atm}$)

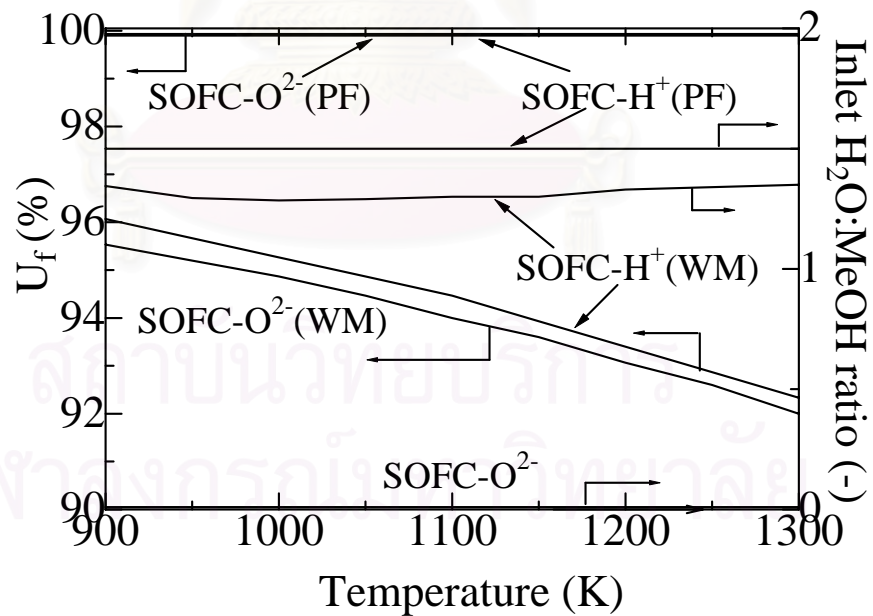


Fig.5.4. Operating conditions corresponding to those in Fig. 5.5, at maximum efficiency ($P = 1 \text{ atm}$)

5.4 Conclusions

The performance of methanol-fuelled SOFCs using proton- and oxygen ion-conducting electrolytes and operating under plug flow and mixed flow modes is investigated. The electromotive force and efficiency are dependent on fuel utilization, inlet H₂O: MeOH ratio, operating temperature, mode of operation and electrolyte type. The benefit of less steam requirement for the SOFC-O²⁻ is taken into account in comparisons of SOFC performance. It is demonstrated that the plug flow is superior to the mixed flow and that the use of the proton-conducting electrolyte is more preferable.



สถาบันวิทยบริการ
จุฬาลงกรณ์มหาวิทยาลัย

CHAPTER VI

BENEFIT OF INCORPORATING PALLADIUM MEMBRANE REACTOR IN SOLID OXIDE FUEL CELL SYSTEM

Summary

In this chapter, the benefit of palladium membrane reactor on SOFC system is concerned. The investigation is divided into two parts: 1) the characteristics of SOFC system and their influences of operating parameter on the performance of SOFC system 2) the preliminary study of SOFC system when operated with a palladium membrane reactor. The performance of the former SOFC system and the latter one was also compared in the study.

The results indicate that SOFC performance depends on fuel utilization and operating temperature. Applying palladium membrane reactor to an SOFC system gains the benefit over the conventional SOFC system due to a smaller SOFC stack at the same electrical power. It was found that the performance of SOFC system integrated with a membrane reactor is significantly dependent on the operating hydrogen recovery of the membrane reactor. The more hydrogen recovery, the higher SOFC performance is gained.

สถาบันวิทยบริการ
จุฬาลงกรณ์มหาวิทยาลัย

6.1 SOFC model

An SOFC consists of two porous ceramic electrodes (e.g. an anode and a cathode), a solid ceramic electrolyte and an interconnect. Typical SOFC materials are stabilized zirconia (Y_2O_3 stabilized ZrO_2 ; YSZ) for electrolyte, nickel/zirconia (Ni- ZrO_2) cermet for anode, and doped lanthanum manganite ($LaSrMnO_3$; LSM) for cathode. The theoretical open-circuit voltage is the maximum voltage under specific operating conditions. Several losses are common to all types of fuel cell. The voltage drop was caused by three major irreversibilities, i.e., ohmic overpotential, activation overpotential and concentration overpotential. The actual voltage can be express as follows:

$$V = E_0 - (\eta_{ohm} + \eta_{Act,a} + \eta_{Act,c} + \eta_{Conc,a} + \eta_{Conc,c}) \quad (2.8)$$

where E_0 is open circuit voltage determined by Eq. 2.7 and η_i is type of overpotential in the SOFC cell.

Ohmic Overpotential (Ohm)

The ohmic loss is the major loss mechanism in an electrolyte-supported fuel cell (Hernandez-Pacheco, *et al.*, 2004). Ohmic polarization obeys Ohm's law and is given by

$$\eta_{Ohm} = iR_j \quad (6.1)$$

The resistance of material can be calculated from respective resistivity which is the function of temperature (Bessette, *et al.*, 1995).

$$R_j = \frac{\rho \delta}{A} \quad (6.2)$$

where $\rho = a_o e^{(b_o/T)}$; a_o and b_o are the constant values depending on type of material and their values are given in Table D1 (in App. D).

Activation Overpotential (*Act*)

Activation overpotential represents the kinetic of reactions taking place on the electrode surface (e.g. anode and cathode). The activation overpotential can be calculated by Eq 6.3 and 6.4 (Achenbach, 1994). It should be noted that these resistances are assumed not to be dependent on current density.

$$\tilde{R}_{Act,c,O_2} = \left[\frac{4F}{RT} k_{O_2} (p_{O_2,c})^{m_{O_2}} \exp\left(-\frac{E_{A,pol,O_2}}{RT}\right) \right]^{-1} \quad (6.3)$$

$$\tilde{R}_{Act,a,H_2} = \left[\frac{2F}{RT} k_{H_2} (p_{H_2,a})^{m_{H_2}} \exp\left(-\frac{E_{A,pol,H_2}}{RT}\right) \right]^{-1} \quad (6.4)$$

where the constants are shown in Table D2 (in App. D)

Concentration Overpotential (*Conc*)

The main factors that contribute to concentration polarization are diffusion of gases through the porous media. In this work, it is assumed that the concentration overpotential is negligible. This assumption is valid as long as the current density is not very high (Pfafferodt *et al.*, 2005).

6.2 Solid oxide fuel cell system

A conventional SOFC system consists of a SOFC unit, a reformer, a afterburner, and pre-heaters (as illustrated in Fig. 6.1). Fuel (methanol) and water are mixed and heated in Pre-heater 1 before entering the reformer. The gas mixture from the reformer enters in the anode compartment of the SOFC where hydrogen reacts with oxygen ions passing through the solid electrolyte. Hydrogen is not completely consumed within the SOFC cell in order to avoid dramatic losses in the electric potential of the SOFC. The exhaust gases from SOFC unit are fed to the afterburner. The combustion heat from the afterburner is then supplied to the endothermic sections by using two unit exchangers (Pre-heat I and II). Table 6.1 summarized a standard operating condition of the conventional SOFC system.

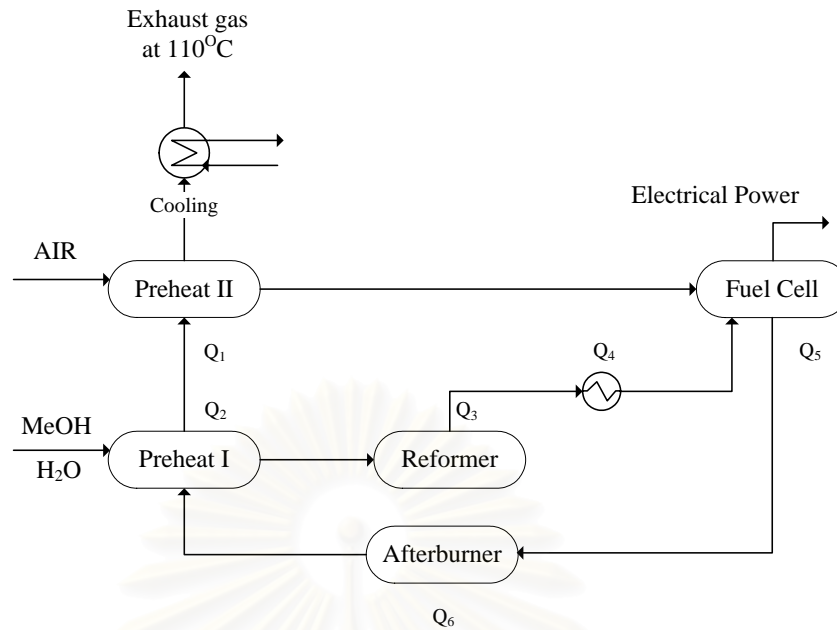


Fig. 6.1 A conventional solid oxide fuel cell systems

For the second SOFC system, a palladium membrane reactor is employed to SOFC system. Fig. 6.2 shows the schematic diagram of this system. Inside a membrane reactor, two sections are divided, e.g., the reaction zone and the purification zone. In the reaction zone, the reforming reactions take place. The produced hydrogen in the reaction zone is extracted in the purification zone and then fed to the SOFC unit. It is expected that the performance of SOFC unit fed with high purity of hydrogen will be superior to that of the conventional one. The effluent gases from the membrane reactor and SOFC unit are combusted in the burner. The combustion heat is provided to the equipments in the system. Table 6.1 presents the standard operating condition of the SOFC system with palladium membrane reactor.

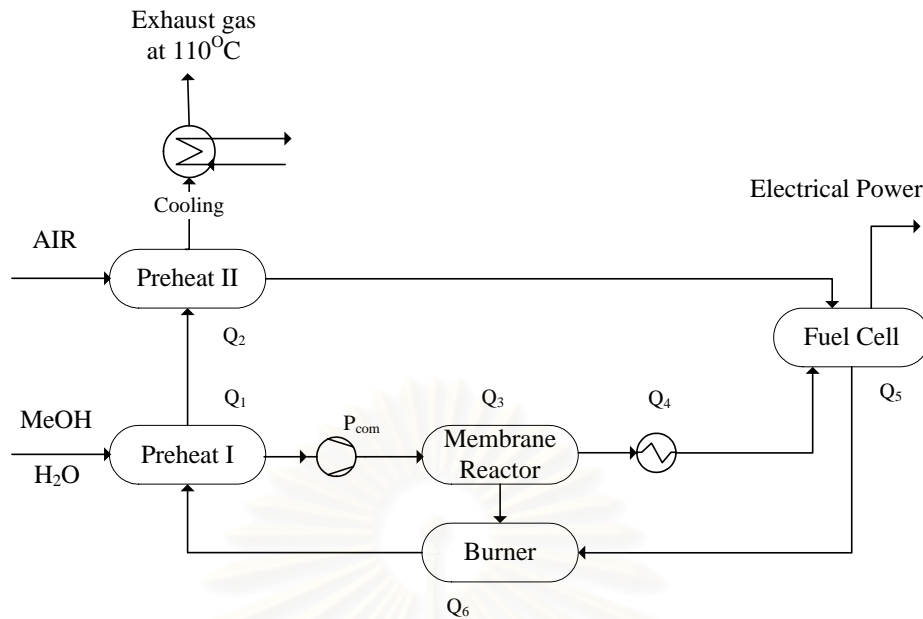


Fig. 6.2 A solid oxide fuel cell system integrated with a membrane separation unit

6.2.1 Reformer

The reformer is the unit for converting methanol to hydrogen by steam reforming reaction. It should be noted that the assumption of the equilibrium state of gas compositions along the flow channel may be reasonable because the rates of methanol steam-reforming and the water gas shift reaction are fast, particularly at high temperature (Pakornphant *et al.*, 2004). Several researchers reported that the conversion of methanol from the methanol steam-reforming always close to 100 % when the operating temperature above 623 K is applied (Amandusson and Ekedahl, 1999). The chemical reactions in the reformer are presented as follows:



From Fig. 6.1, the fuel mixed gases (methanol and steam) were entered in the reformer. The reforming temperature is operated at 973 K. The heat involving reactions in the reformer (Q_3) can be calculated from heat of reaction (3.1) to (3.3). It

is assumed that the reformer is operated under isothermal condition. The temperature of leaving gases is equal to the operating temperature of the reformer.

6.2.2 Solid oxide fuel cell

For an SOFC unit, it is common to assume that only H₂ is oxidized via electrochemical reaction. All reactions in the SOFC unit are assumed to be in equilibrium. The net heat of this unit (Q_5) is defined as the summation of electrical power and the heat released by enthalpy change of hydrogen oxidation. The electrical power can be calculated by Eq. 6.5.

$$\text{Electrical power} = \text{Current} \times \text{Operating Voltage} \quad (6.5)$$

Generally, the SOFC is not operated at the maximum power due to low efficiency. The SOFC was suggested to operate at the relative power of 0.7 (Demin *et al.*, 2004). It should be noted that the relative power is defined as the ratio of power to the maximum achievable power at the specific condition. The fuel cell operation at lower power is attractive from the point of view that the higher efficiency is obtained. However, too low power is not pleasant due to high cost of SOFC cell.

6.2.3 Afterburner

The depleted fuel gases from the anode and the depleted air from the cathode was fed to an afterburner. The remaining H₂, CO, CH₄ and methanol in the anode effluent will react with oxygen in the depleted air of SOFC. The oxidation reaction in the afterburner is assumed as reaching completion (100% conversion) (Zhang *et al.*, 2005). The combustion heat (Q_6) is then provided to other equipments (i.e. preheating unit for methanol, steam and air) in the SOFC system.

6.2.4 Compression unit

This unit is used for increasing driving force in palladium membrane reactor. Increasing the operating pressure can significantly improve the hydrogen permeation flux across the palladium membrane (Lin *et al.*, (2003)). Peppley *et al.* (1999)

considered in methanol steam reforming reaction system over a wide range of temperature (up to 533 K) and total pressure (39 bar). It was found that methanol conversion will be extended with increasing reaction. Required power in this unit (P_{com}) is determined from following Eq:

$$P_{com} = f \times (p_2 - p_1) \quad (6.6)$$

where f is volumetric flow rate, 2 and 1 are represented retentate and permeate side of palladium membrane respectively.

Table 6.1 Operating condition

	Case I	Case II
Inlet H ₂ O: MeOH ratio	1	1
Fuel Utilization	80 %	80%
<i>Unit of operation</i>		
reformer	973 K and 1 atm	-
Palladium membrane reactor	-	973 K and 20 atm
SOFC	1173 K and 1 atm	1173 K and 1 atm
Afterburner	1173 K	1173 K

6.2.5 Net heat (Q_{net})

This value is the total heat of system which is one of performance indicators used in this work. The total heat of system (Q_{net}) can be defined as a following equation:

$$Q_{net} = Q_1 + Q_2 + Q_3 + Q_4 + Q_5 + Q_6 \quad (6.7)$$

where Q_i is power consumption/generation in each unit (kW).

6.3 Palladium membrane reactor

Membrane reactor was developed to combine the reaction and purification in one system. The reaction product can be removed directly from the reaction zone by selective membrane. Therefore, the reaction can be carried out even at low reaction temperature while still achieving high conversion. In lots of hydrogen-containing systems, supported palladium membranes were commonly used as the hydrogen-permeable membrane (Kikuchi, 2000).

In this work, palladium membrane thickness was chosen at 10 μm . due to their minimum in the palladium material cost, defects and manufacturing difficulties of a thinner membrane (Dittmeyer *et al.*, 2001).

The hydrogen flux through a palladium membrane is typically limited by the diffusion of hydrogen atoms through the membrane film, in which the flux can be represented by Eq.6.8

$$\bar{N}_{H_2} = \frac{Q_0}{\delta} \exp\left(\frac{-E_D}{RT}\right) (p_{H_2,r}^{0.5} - p_{H_2,p}^{0.5}) \quad (6.8)$$

where δ is the membrane thickness and driving force is proportional to the difference in the square roots of the hydrogen partial pressure on the retentate and permeate sides of the membrane reactor. The resistance of the porous support is negligible. The parameters of Eq. 6.8 are presented in Table E1 (see in APP. E). Area of palladium membrane reactor can be calculated from average hydrogen flux through membrane by a following equation:

$$Area_{Mem} = \frac{\text{molar flowrate of } H_2 \text{ recovery}}{\bar{N}_{H_2}} \quad (6.9)$$

where \bar{N}_{H_2} is the average hydrogen flux through palladium membrane

6.4 Results and discussion

6.4.1 Performance of SOFC unit

In operation, hydrogen in the fuel is consumed along the fuel channel by the electrochemical reaction. Fig. 6.3 illustrates typical characteristic curves of SOFC unit. When the cell is operated at higher current density the cell voltage decreases due to the increased irreversible losses whereas the power density increases initially and then decreases. Therefore, the current density should be carefully selected to achieve a maximum power density. The results also reveal that the fuel utilization influences the characteristic curves. At high value of fuel utilization, the hydrogen concentration in the anode fuel channel becomes more depleted and therefore lower cell voltage and power density can be obtained. The effect of operating temperature on the cell performance is illustrated in Fig. 6.4. Higher cell performance can be achieved at higher operating temperature due to significant reduction of cell resistances. The maximum power density and its corresponding electrical efficiency at different fuel utilization and temperature are provided in Fig.6.5. It is obvious that the operation at higher fuel utilization results in higher electrical efficiency but higher cell area is required due to the lower power density. In addition, high operating temperature is always favorable operating condition; however, the presence of some technical constraints, such as limits the use of the availability of seal cell at high temperature. The operating temperature of 1173 K will be used in the following studies of this thesis.

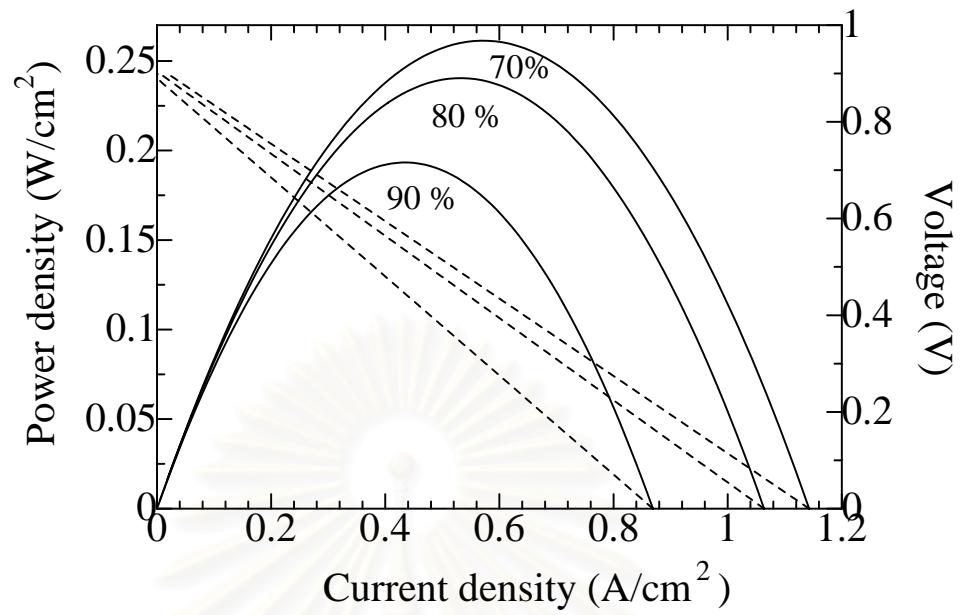


Fig.6.3 Performance characteristics for comparison effect of fuel utilization at inlet $\text{H}_2\text{O}:\text{MeOH} = 1$ and $T = 1173 \text{ K}$ (Solid lines represent power density, Dash lines represent voltage)

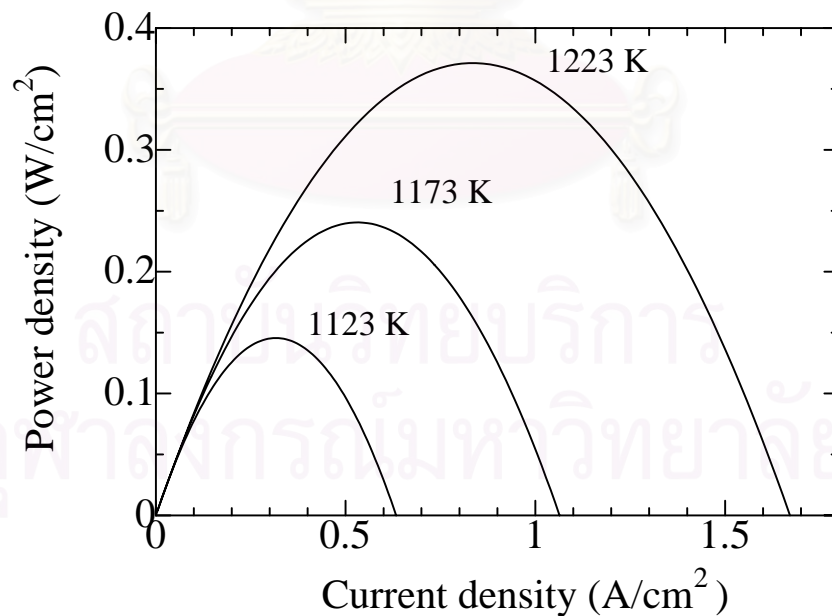


Fig.6.4 Performance characteristics for comparison effect of fuel cell temperature at inlet $\text{H}_2\text{O}:\text{MeOH} = 1$ and $U_f = 80 \%$

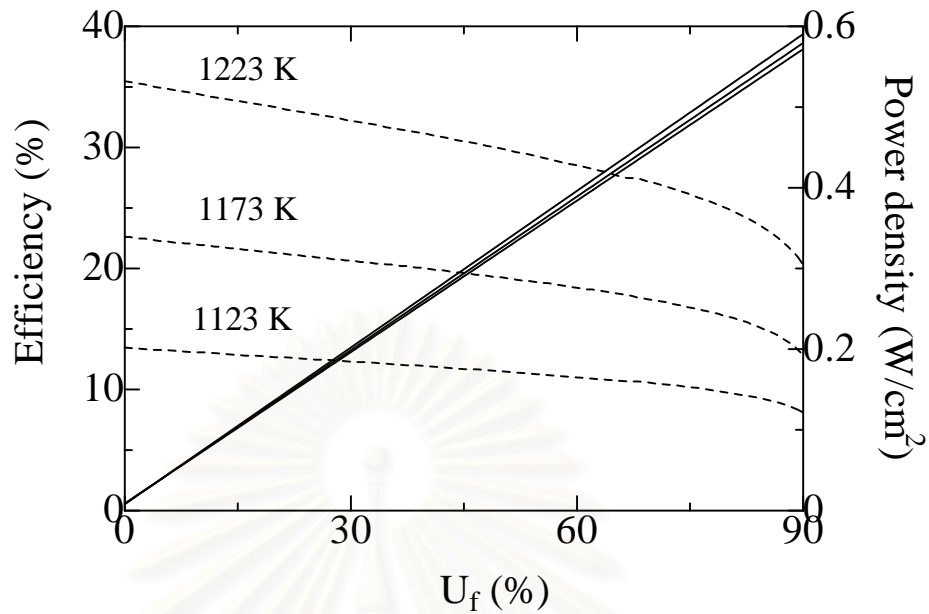


Fig.6.5 Performance of SOFC at maximum power density for comparison effect of fuel utilization and operating temperature at inlet $H_2O: MeOH = 1$ (Solid lines represent efficiency, Dash lines represent power density)

6.4.2 Performance comparison between with and without membrane reactor

6.4.2.1 Effect of operating pressure of membrane reactor on hydrogen recovery

Operating pressure of the reaction chamber in the membrane reactor is an important parameter determining the hydrogen recovery obtained in the permeate side. Hydrogen partial pressure in the reaction chamber higher than that of the permeate side (1 atm) is required to allow hydrogen to transport through the membrane. Fig. 6.6 shows that at low hydrogen recovery (< 70 %) a slight increase of pressure can significantly improve the hydrogen recovery. However, much higher pressure is essential to achieve high hydrogen recovery. On the other words, compression cost dramatically increases hydrogen recovery. The hydrogen recovery of 80, 85 and 90% required the pressure at least 8, 11, 19 atm, respectively.

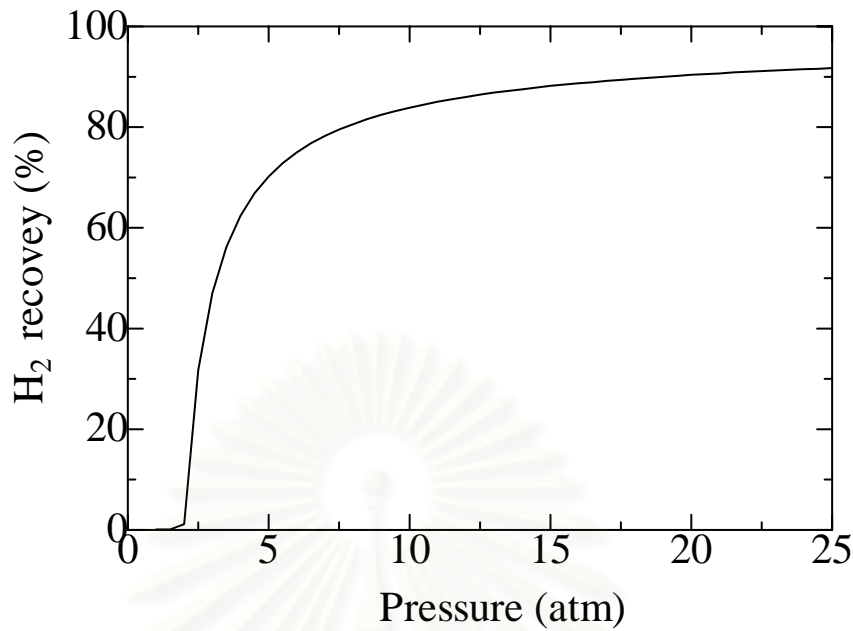


Fig.6.6 Effect of pressure on hydrogen recovery by Pd membrane at inlet H₂O: MeOH = 1, $U_f = 80\%$ and $T = 1173\text{ K}$

6.4.2.2 Effect of hydrogen recovery on performance of SOFC unit

In Section 6.4.1, the performance of SOFC unit with the hydrogen rich feed from conventional reformer was determined. When the membrane reactor is integrated to the SOFC system, the SOFC unit is operated with pure hydrogen. Fig. 6.7 shows the characteristic curves of the SOFC unit fed with different feeds. The cell operating at $T = 1173\text{ K}$ and fuel utilization (U_f) of 80%. Dashed line shows the power density for the case with the feed from the conventional reformer. It is obvious that the level of hydrogen recovery significantly influences the performance of the cell. The hydrogen recovery must be sufficiently high to offer superior performance to the case with conventional reformer. The maximum power density increases from 0.240 Wcm^{-2} for the conventional to 0.247 and 0.268 Wcm^{-2} , for the SOFC system with hydrogen recovery of 85 and 90%, respectively, due to the increase of hydrogen concentration in feed. When the system is operated at constant fuel utilization, the hydrogen concentration along the fuel channel is governed by the hydrogen recovery. At low hydrogen recovery, the fuel depletion near the exit of the SOFC unit deteriorates the SOFC performance as observed by the reduction of power density. From this study, it is obvious that the hydrogen recovery is an important factor which

determines whether the inclusion of the membrane reactor in the SOFC system is the benefit to the SOFC performance.

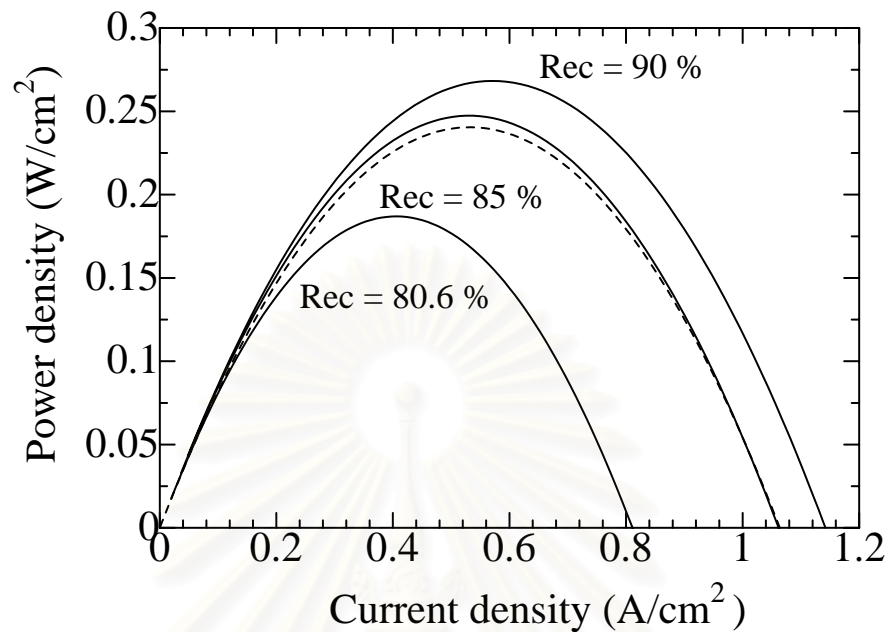


Fig.6.7 Performance characteristics for comparison effect of hydrogen recovery at inlet $H_2O: MeOH = 1$, $U_f = 80\%$, $T = 1173\text{ K}$ (Dashed line represents conventional SOFC system and solid lines represent SOFC system plus separation unit)

6.4.2.3 Benefit from the use of membrane reactor in the SOFC system

In order to determine the benefit from the use of palladium membrane reactor in the SOFC system, the calculations base on two cases; i.e. conventional SOFC system (case I) and SOFC system with palladium membrane reactor (case II) were carried out. For both cases the SOFC unit is operated at $T = 1173\text{ K}$ and $U_f = 80\%$. Table 6.2 summarizes the results of both cases. For the conventional SOFC system (case I), the SOFC unit is operated at 0.63 V which provides the power density of 0.7 time of the maximum power density recommended in the literature (Demin *et al.*, 2004). The system offers the electrical efficiency of 34.47% and the power density of 0.203 Wcm^{-2} . For the system with membrane reactor (case II), the membrane reactor is operated at 90% hydrogen recovery and the operating voltage was carefully selected so that the net electrical efficiency is equal to that of case I. Note that an additional electrical power of 17.25 kW is generated in the SOFC unit to operate the

compressor for operating the membrane reactor at elevated pressure (20 atm). In addition, for both systems, the exothermic heat (Q_5 and Q_6) can sufficiently provide to the endothermic heat (Q_1 , Q_2 , Q_3 and Q_4). From the results, it is obvious that the use of the membrane reactor allows the SOFC unit to operate at higher power density and therefore smaller SOFC cell area is required. Preliminary economic analysis for these cases indicates that when the membrane reactor is used in the system, the SOFC cell area of 3.55 m^2 can be reduced which is equal to 5,325 US\$; however, the membrane area of 67.79 m^2 is required for the membrane reactor which is equal to 50,571 US\$. According to the present approximate cost of the SOFC cell (1500 US\$/ m^2 from Riensche *et al.*, 1998) and palladium membrane (746 US\$/ m^2 from New York Mercantile Exchange market and Criscuoli *et al.*, 2001), the use of the palladium membrane reactor is still not economical. The reduction of palladium membrane cost to 78.77 US\$/ m^2 is important to make the SOFC system with membrane reactor become economical. It should be noted that the previous calculations neglect the cost and efficiency of the compressor. Therefore, they must be taken into account in the detailed analysis.

Fig.6.8 shows the effect of the hydrogen recovery on the reduction of SOFC cell area and the required membrane area. As expected, the higher the hydrogen recovery, the higher reduction of SOFC cell area and the higher the required membrane area.

Table 6.2 Results of simulation

		Power consumption in each unit	
		Case I	Case II
<i>Stack data</i>			
Fuel utilization (U_f)	%	80.00	80.00
Cell Voltage	V	0.63	0.655
Current density	A/cm ²	0.322	0.346
Power density	W/cm ²	0.203	0.227
Cell Area	m ²	108.27	104.72
<i>Palladium membrane</i>			
% recovery	%	-	90.00
Membrane area	m ²	-	67.89
<i>Power production</i>			
Electrical power	kW	220.00	237.25
Afterburner (Q_6)	kW	986.70	977.00
<i>Power consumption</i>			
Preheat I (Q_1)	kW	598.50	598.50
Preheat II (Q_2)	kW	227.25	227.25
Reformer or Membrane reactor (Q_3)	kW	81.95	77.57
Preheat III (Q_4)	kW	27.79	28.84
Compression process (P_{com})	kW	-	17.25
<i>Net heat</i>	kW	469.53	426.65
<i>Net Electrical efficiency</i>	%	34.47	34.47

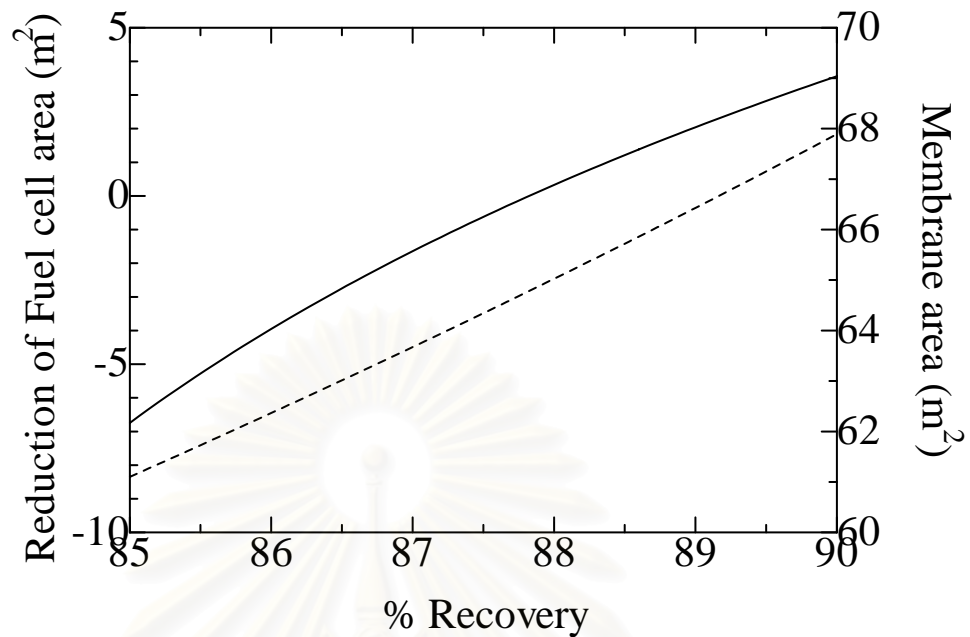


Fig.6.8 Effect of hydrogen recovery on reduction of fuel cell area (solid line) and membrane area (dashed line) at inlet $\text{H}_2\text{O}:\text{MeOH} = 1$, $U_f = 80\%$ and $T = 1173\text{ K}$

6.5 Conclusions

The profit of a purified hydrogen unit in SOFC system for the production of electricity from methanol steam reforming reaction is described. First analysis is concerned on conventional SOFC system. It shows that fuel utilization can improve fuel cell efficiency but reduce performance characteristics.

Second analysis is considered on the benefit from palladium membrane reactor on SOFC unit. It is found that the fuel cell area can be reduced 3.56 m^2 by using palladium membrane reactor which has the area is 67.79 m^2 for 90% recovery. Thus the use of the palladium membrane reactor is still not economical. The palladium membrane cost should be reduced to $78.77\text{ US\$/m}^2$ is for economical propose.

In the basic concept, palladium membrane has more interesting for improving the fuel cell performance but it does not make any benefit in term of economic.

CHAPTER VII

CONCLUSIONS AND RECOMMENDATIONS

7.1 Conclusions

This thesis involves in performance analysis of SOFC system fed by methanol. It consists of three parts, that is, determination of boundary of carbon formation with different types, theoretical performance analysis with different electrolyte and investigation on benefit of incorporating palladium membrane reactor in SOFC system. The following conclusions can be drawn:

1. A theoretical thermodynamic analysis has been performed to predict the boundary of carbon formation for a SOFC with direct internal reforming. The results indicate that carbon formation can be protected by increasing inlet H₂O: MeOH ratio or increasing the operating temperature. SOFC-O²⁻ is more preferable than SOFC-H⁺ in term of lower steam requirement in the feed.

2. The theoretical performance of methanol-fuelled SOFC using proton- and oxygen ion- conducting electrolytes and operated under plug flow and mixed flow modes is investigated. The results indicate that the electromotive force and theoretical efficiency are depended on fuel utilization, inlet H₂O: MeOH ratio, operating temperature, operating mode and electrolyte type. Although SOFC-O²⁻ can gain benefit from the lower steam requirement, its theoretical efficiency is still lower than SOFC-H⁺.

3. The results indicate that the use of palladium membrane reactor allows the SOFC system to operate with smaller SOFC stack to achieve the equivalent electrical power of the conventional system. However, it is significantly depend on the operating hydrogen recovery.

7.2 Recommendations

1. It should be realized that carbon may be formed by the other mechanisms besides the Boudard reaction and the decomposition of methane. Moreover, other forms of carbonaceous species such as polymeric coke (C_nH_m), which can also result in comparable damage, can exist in the system. Therefore, the results obtained here should be considered only as crude guideline for the operating conditions of a SOFC. Experimental work, including a kinetic study of the rate of carbon formation, should be carried out to determine the most suitable inlet H_2O : MeOH ratio.

2. SOFC- O^{2-} has more benefit than SOFC- H^+ in case of inlet steam: fuel requirement for prevention carbon formation but SOFC- H^+ has higher theoretical efficient. Because in the theoretical calculation, the actual losses for both electrolytes have not been taken into account, further study is required to compare the actual performance among both systems.

3. Palladium membrane reactor can improve performance of SOFC but it increases cost of operation and cost of palladium membrane. The results show that the cost of palladium membrane area reduces approximately ten times for economical. For advantage, other information is necessary for that calculation.

REFERENCES

- Achenbach, E. Three-Dimensional and Time-Dependent Simulation of a Planar Solid Oxide Fuel Cell Stack. *Journal of Power Sources* **49** (1994): 333-348.
- Aguiar, P. Modeling Studies of Solid Oxide Fuel Cells with Internal Methane Steam Reforming. Ph.D. Thesis, University of London, UK, 2002.
- Aguiar, P., C.S. Adjiman, and N.P.Brandon. Anode-supported intermediate temperature direct internal reforming solid oxide fuel cell. I: model-based steady -state performance. *Journal of Power Sources* **138** (2004): 120-136.
- Aguiar, P., D. Chadwick and L. Kershenbaun. Modelling of an Indirect Internal Reforming Solid Oxide Fuel Cell. *Chemical Engineering Science* **57** (2002): 1665-1677.
- Ahmed, S. and M.Krumpelt Hydrogen from hydrocarbon fuels for fuel cells. *Journal of Hydrogen Energy* **26** (2001) 291-301.
- Amanduson, H., L.G. Ekedahl and H. Dannelun. Methanol-induced hydrogen permeation through a palladium membrane. *Surface Science* **442** (1999): 199-205.
- Amphlett J.C., M.J.Evans, R.A.Jones, R.F.Mann, R.D.Weir. Hydrogen production by the catalytic steam reforming of methanol, Part 1: Thermodynamics. *Canadian Journal of Chemical Engineering* **59** (1981): 720-727.
- Amphlett J.C., R.F.Mann, R.D.Weir. Hydrogen production by the catalytic steam reforming of methanol. Part 3: Kinetics of methanol decomposition using $C_{18}HC$ catalyst. *Canadian Journal of Chemical Engineering* **66** (1988): 950-956.
- Assabumrungrat, S., V. Pavarajarn, S. Charojrochkul and N. Laosiripojana. Thermodynamic analysis for a solid oxide fuel cell with direct internal reforming fueled by ethanol. *Chemical Engineering Science* **59** (2004): 6015-6020.
- Badwal, S.P.S., and K.Foger. Solid Oxide Fuel Cell Review. *Ceramics International* **22** (1996): 257-265.
- Bedringas, Kai W., Ivar S. Ertesvag, Stale Byggstotl, and Bjorn F. Magnussen. Exergy analysis of solid oxide fuel cell (SOFC) systems. *Energy* **22** (1997): 403-412.

- Bessette, N.F., W.J. Wepfer and J. Winnick;. A Mathematical Model of a Solid Oxide Fuel Cell. *Journal of the Electrochemical Society* **142** (1995): 3792-3800.
- Braun, R.J., S.A. Klein, D.T. Reindl. Evaluation of system configurations for solid oxide fuel cell-based micro-combined heat and power generators in residential applications. *Journal of Power Sources* article in press (2005).
- Brown, L.F. A comparative study of fuels for on-board hydrogen production for fuel-cell-powered automobiles. *Journal of Hydrogen Energy* **26** (2001): 381-397.
- Buxbaum, R.E. and A.B. Kinney. Hydrogen transport through tubular membranes of palladium-coated tantalum and niobium *Industrial and Engineering Chemistry* **35** (1996): 530-537.
- Chan, S.H., C.F. Low, O.L. Ding. Energy and exergy analysis of simple solid-oxide fuel-cell power systems. *Journal of Power Sources* **103** (2002): 188-200.
- Chan, S.H., and O.L.Ding. Simulation of a solid oxide fuel cell power system fed by methane. *Journal of Hydrogen Energy* **30** (2005): 167-179.
- Clarke, S.H., A. L. Dicks, K. Pointon, T. A. Smith and A. Swann. Catalytic aspects of the steam reforming of hydrocarbons in internal reforming fuel cells. *Catalysis Today* **38** (1997): 411-423.
- Costamagna, P., Azra Selimovic, Marco Del Borghi, and Gerry Agnew. Electrochemical model of the integrated planar solid oxide fuel cell (IP-SOFC). *Chemical Engineering Journal* **102** (2004): 61-69.
- Coutelieris, F.A., S.L.Douvartzides, and P.E.Tsiakaras. The importance of the fuel choice on the efficiency of a solid oxide fuel cell system. *Journal of Power Sources* **123** (2003): 200-205.
- Coutelieris, F.A., S.L.Douvartzides, and P.E. Tsiakaras. The importance of the fuel choice on the efficiency of a solid oxide fuel cell system. *Journal of Power Sources* **123** (2003): 200-205.
- Criscuoli, A., A. Basile, E. Drioli, O. Loiacono. An economic feasibility study for water gas shift membrane reactor. *Journal of Membrane Science* **181** (2001): 21-27.
- Demin, A.K., and P.Tsiakaras. Thermodynamic analysis of a hydrogen fed solid oxide fuel cell based on proton conductor. *Journal of Hydrogen Energy* **26** (2001): 1103-1108.

- Demin, A.K., P.Tsiakaras, V.A. Sobyenin and S.Hramova. Thermodynamic analysis of a methane fed SOFC system based on protonic conductor. *Solid State Ionics* **152-153** (2002): 555-560.
- Demin, A.K., P.Tsiakaras, E.Gorbova and S.Hramova. A SOFC base on a co-ionic electrolyte. *Journal of Power Sources* **131** (2004): 231-236.
- Dicks, A. L. Advances in catalysts for internal reforming in high temperature fuel cells. *Journal of Power Sources* **71** (1998): 111-122.
- Dittmeyer, R., V. Hollein, K. Daub. Membrane reactors for hydrogenation and dehydrogenation processes based on supported palladium. *Journal of Molecular Catalysis A: Chemical* **173** (2001): 135-84.
- Douvartzides, S., F.Coutelieris, and P.Tsiakaras. Exergy analysis of a solid oxide fuel cell power plant fed by either ethanol or methane. *Journal of Power Sources* **131** (2004): 224-230.
- Douvartzides, S., F.Coutelieris, and P.Tsiakaras. On the systematic optimization of ethanol fed SOFC-based electricity generating systems in term of energy and exergy. *Journal of Power Sources* **114** (2003): 203-212.
- Douvartzides, S.L., F.A. Coutelieris, A.K. Demin, and P.E. Tsiakaras. Fuel options for Solid Oxide Fuel Cells: a thermodynamic Analysis. *ALChE Journal* **49** (2003): 248-257.
- Finnerty, C M. and R. Mark Ormerod. Internal reforming over nickel/zirconia anodes in SOFCs operating on methane: influence of anode formulation, pre-treatment and operating conditions. *Journal of Power Sources* **86** (2000): 390-394.
- Finnerty, C M., Neil J. Coe, Robert H. Cunningham and R. Mark Ormerod. Carbon formation on and deactivation of nickel-based/zirconia anodes in solid oxide fuel cells running on methane. *Catalysis Today* **46** (1998): 137-145.
- Galvita, V.V., V.D.Belyaev, A.V.Frumin, A.K.Demin, P.Tsiakaras and V.A. Sobyenin. Performance of a SOFC fed by ethanol reforming products. *Solid State Ionics* **152-153** (2002): 551-554.
- Gorte, R. J., S.Park, J.M. Vohs, C. Wang. Anodes for direct oxidation of dry hydrocarbons in a solid-oxide fuel cell. *Advanced Materials* **12** (2000): 1465-1469.

- Hernandez-Pacheco E., D. Singh, P. N. Hutton, N. Patel, M. D. Mann. A macro-level model for determining the performance characteristics of solid oxide fuel cells. *Journal of Power Sources* **138** (2004): 174–186.
- Hirschenhofer, J.H., D.B. Stauffer, R.R. Engleman and M.G. Klett. Fuel Cell Handbook, 4th edition, *Parsons Corporation Reading, USA*, 1998.
- Hollock, G.L.. Diffusion and solubility of hydrogen in palladium and palladium-silver alloy. *Journal of Physical Chemistry* **74** (1970): 503-511.
- Iora, P., P.Aguiar, C.S. Adjiman, and N.P.Brandon. Comparison of two IT DIR-SOFC models: Impact of variable thermodynamic, physical, and flow properties. Steady-state and dynamic analysis. *Chemical Engineering Science* **60** (2005): 2963-2975.
- Jarosch, K., and H.I. de Lasa. Permeability, Selectivity, and Testing of Hydrogen Diffusion Membranes Suitable for Use in Steam Reforming. *Industrial and Engineering Chemistry Research* **40** (2001): 5391-5397.
- Kikuchi, E.. Membrane reactor application to hydrogen production. *Catalysis Today* **56** (2000): 97-101.
- Koh, J.H., A.T. Hsu, H.U. Akay, and M.F. Liou. Analysis of overall heat balance in self-heated proton-exchange-membrane fuel cells for temperature prediction. *Journal of Power Sources* article in press (2005).
- Larinie, J. and A.Dicks. Fuel Cell System Explained. *John Wiley & Sons, New York* 2000.
- Lattner, J.R., and M.P. Harold. Comparison of conventional and membrane reactor fuel processors for hydrocarbon-based PEM fuel cell systems. *International journal of Hydrogen Energy* **29** (2004): 393-417.
- Lin, Y.M., S.L. Liu, C.H. Chuang and Y.T. Chu. Effect of incipient removal of hydrogen through palladium membrane on the conversion of methane steam reforming Experimental and modeling. *Catalysis Today* **82** (2003): 127-139.
- Lwin, Y., W.R.W. Daud, A.B. Mohamad, and Z. Yaakob. Hydrogen production from steam-methanol reforming: thermodynamic analysis. *Journal of Hydrogen Energy* **25** (2000): 47-53.
- Matelli, Jose Alexandre, and Edson Bazzo. A methodology for thermodynamic simulation of high temperature, internal reforming fuel cell systems. *Journal of Power Sources* **142** (2005): 160-168.

- Matsuzaki Y., I. Yasuda. The poisoning effect of sulfur-containing impurity gas on a SOFC anode Part I. Dependence on temperature, time, and impurity concentration. *Solid State Ionics* **132** (2000): 261–269.
- Monanteras, N. C., C. A. Frangopoulos. Towards synthesis optimization of a fuel-cell based plant. *Energy Conversion & Management* **40** (1999): 1733-1742.
- Nagata, S., Akihiko Momma, Tohru Kato, and Yasuhiro Kasuga. Numerical analysis of output characteristics of tubular SOFC with internal reformer. *Journal of Power Sources* **101** (2001): 60-71.
- Pacheco, E.H., D. Singh, P. N. Hutton, N. Patel, M.D. Mann. A macro-level model for determining the performance characteristics of solid oxide fuel cells. *Journal of Power Sources* **138** (2004): 174–186.
- Pakornphant, C. C. Sumaeth, S. Johannes. Temperature-programmed desorption of methanol and oxidation of methanol on Pt-Sn/Al₂O₃ catalysts. *Chemical Engineering Journal* **97** (2004): 161-171.
- Park, S., R. J. Gorte and J. M. Vohs. Applications of heterogeneous catalysis in the direct oxidation of hydrocarbons in a solid-oxide fuel cell. *Applied Catalysis A* **28** (2000): 55-61.
- Peppley, B.A., J.C. Amphlett, L.M. Kearns, R.F. Mann. Methanol steam reforming on Cu/ZnO/Al₂O₃ Part 1: the reaction network. *Applied Catalysis A* **179** (1999): 21-29.
- Pfafferodt M., P. Heidebrecht, M. Stelter, K. Sundmacher. Model-based prediction of suitable operating range of a SOFC for Auxiliary Power Unit. *Journal of Power Sources* **140** (2005): 53-62.
- Riensch E., U. Stimming and G. Unverzag. Optimization of a 200 kW SOFC cogeneration power plant Part I: Variation of process parameters. *Journal of Power Sources* **73** (1998): 251–256.
- Rostrup-Nielsen, R. Jen. Conversion of hydrocarbons and alcohols for fuel cells. *Physical Chemistry Chemical Physics* **3** (2001): 283-288.
- Trimm, D.L.. Catalysts for the control of coking during steam reforming. *Catalysis Today* **49** (1999): 3-10.
- Tsiakaras, P., and A.K. Demin. Thermodynamic analysis of a solid oxide fuel cell system fuelled by ethanol. *Journal of Power Sources* **102** (2001): 210-217.
- Wild, P.J. and M.J.F.M. Verhaak. Catalytic production of hydrogen from methanol. *Catalysis today* **60** (2000): 3-10.

- Williams M.C., J.P. Strakey, W.A. Surdoval. The U.S. Department of Energy, Office of Fossil Energy Stationary Fuel Cell Program. *Journal of Power Sources* **143** (2005): 191–196.
- Yamamoto, O. Solid Oxide Fuel Cells: Fundamental Aspect and Prospects. *Electrochim. Acta* **45** (2000): 2423-2435.
- Zhang, W., E.Croiset, P.L. Douglas, M.W.Fowler, and E.Entchev. Simulation of a tubular solid oxide fuel cell stack using AspenPlus™ unit operation models. *Energy Conversion and Management* **46** (2005): 181–196.



สถาบันวิทยบริการ
จุฬาลงกรณ์มหาวิทยาลัย



APPENDICES

สถาบันวิทยบริการ
จุฬาลงกรณ์มหาวิทยาลัย

APPENDIX A

SELECTED THERMODYNAMIC DATA

Table A1 Heat capacities (C_p)

Components	$C_p = a + bT + cT^2 + dT^3 + eT^4$ [J/mol]				
	a	$b \times 10^3$	$c \times 10^5$	$d \times 10^8$	$e \times 10^{13}$
Methanol	40.046	-38.287	24.529	-21.679	599.09
Methane	34.942	-39.957	19.184	35.103	393.21
Carbon monoxide	29.556	-6.5807	2.0130	-1.2227	22.617
Carbon dioxide	27.437	42.315	-1.9555	0.3997	-2.9872
Water	33.933	-8.4186	2.9906	-1.7825	36.934
Hydrogen	25.399	20.178	-3.8549	3.1880	-87.585
Carbon (s)	-0.8320	34.846	-1.3233	0	0
Carbon (g)	21.069	-0.7920	0.0571	-0.0069	0.0270

Table A2 Heat of formation (H_f), and entropy (S^0)

Components	$H_f = a + bT + cT^2$ [kJ/mol]			S^0 [J/mol.K]
	a	$b \times 10^3$	$c \times 10^5$	
Methanol	-188.19	-49.823	2.0791	239.7
Methane	-63.425	-43.355	1.7220	186.27
Carbon	-112.19	8.1182	-8.0425	197.54
monoxide	-393.42	0.1591	-0.1395	213.69
Carbon dioxide	-241.80	0	0	188.72
Water	0	0	0	130.57
Hydrogen	0	0	0	5.74
Carbon (s)	716.68	0	0	158.1
Carbon (g)				

APPENDIX B

DETERMINING GIBBS ENERGY

B1. Determining Gibbs energy (G) at any temperatures by equations below:

$$G = H - TS \quad (\text{B1})$$

$$dG = dH - d(TS) \quad (\text{B2})$$

Take integration to the equation above:

$$\int dG = \int dH - \int d(TS) \quad (\text{B3})$$

$$G_T - G_{STD} = \int_{298}^T dH - \int_{298}^T d(TS) \quad (\text{B4})$$

Where

$$H = H(T) = a + bT + cT^2 \quad (\text{B5})$$

$$S = S(T) = S^0 + \int_{298}^T C_p dT \quad (\text{B6})$$

Where T = The temperature range of 500 - 1,500 K

S^0 = The entropy at standard state (298 K, 1 atm)

B2. Determining the equilibrium constant (K)

$$G_r = -RT \ln K \quad (\text{B7})$$

Rearrange the above equation;

$$K = \exp\left(-\frac{G_r}{RT}\right) \quad (\text{B8})$$

And from thermodynamic concept

$$K = \prod a_i^{v_i} \quad (\text{B9})$$

For gas phase is considered, we can substitute activity with partial pressure term

$$K = \prod \left(\Phi_i y_i \frac{P}{P^0} \right)^{v_i} \quad (\text{B10})$$

Since it was studied at the pressure of 1 atm, the equation (B10) became the following equation:

$$K = \prod (y_i)^{v_i} \quad (\text{B11})$$

From equation (B11), The converted moles associated to the reactions involved in the production of hydrogen from steam reforming (x_1, x_2, x_3) can be calculated.



สถาบันวิทยบริการ
จุฬาลงกรณ์มหาวิทยาลัย

APPENDIX C

NEWTON'S METHOD

Newton's method is used to solve several unknown answers from equations. This method was applied from Taylor's series expansion to estimate the answers of non-linear equations. The first-order differentiated equations are considered. Then the equation can be applied as follow:

$$f(x+\Delta x) = f(x) + J(x) \Delta x \quad (C1)$$

When $J(x)$ = Jacobian matrix

$$J(x) = \begin{vmatrix} \frac{\partial f_1(x)}{\partial x_1} & \wedge & \wedge & \frac{\partial f_1(x)}{\partial x_n} \\ M & & & M \\ M & & & M \\ \frac{\partial f_n(x)}{\partial x_1} & \wedge & \wedge & \frac{\partial f_n(x)}{\partial x_n} \end{vmatrix} \quad (C2)$$

To solve the answers is to find Δx which providing:

$$0 = f(x) + J(x) \Delta x \quad (C3)$$

Δx is calculated by the linear equation below:

$$J(x) \Delta x = -f(x) \quad (C4)$$

The procedure of the calculation:

1. Set the value of $k = 1$
2. If $k \leq N$ (The largest amount of loops in the operation)
 - 2.1 Find $f(x)$ and $J(x)$
 - 2.2 Solve the equation: $J(x) \Delta x = -f(x)$ to get Δx
 - 2.3 Set $x = x + \Delta x$
 - 2.4 $|f(\Delta x)| < TOLX$ or $|f(x)| < TOLF$, end the calculation
 - 2.5 Set $k = k + 1$ and repeat item 2.1
3. If $i > N$, and the answer hasn't been solved, it would be presumed that the amount of N is too small or the starting value is not appropriate.



สถาบันวิทยบริการ
จุฬาลงกรณ์มหาวิทยาลัย

APPENDIX D

THE CALCULATION OF SOLID OXIDE FUEL CELL SYSTEM

Ohmic overpotentials, which are the specific value of material, are proportion of current density and can be determined by Ohm's Law (Eq.D1)

$$\eta_{Ohm} = iR \quad (D1)$$

The resistance of material can be calculated from respective resistivity which are the function of temperature. (Bessette II *et al.*, 1995)

$$R = \frac{\rho\delta}{A} \quad (D2)$$

Where $\rho = ae^{(b/T)}$; a and b are the constant values depend on type of material and show in Table D1

Table D1 Resistivity and thickness of cell component

Material Used	Ni-YSZ / YSZ / LSM – YSZ
Anode thickness (μm)	150
Anode Ohmic resistance constant	$a = 0.0000298, b = -1392$
Cathode thickness (μm)	$2e-3$
Cathode Ohmic resistance constant	$a = 0.0000811, b = 600$
Electrolyte thickness (μm)	40
Electrolyte Ohmic resistance constant	$a = 0.0000294, b = 10350$
Interconnect thickness (μm)	100
Interconnect Ohmic resistance constant	$a = 0.001256, b = 4690$

Ref. Chan *et al.*, 2002

Activation Overpotentials are consist of 2 parts which are anode and cathode and assume these resistances are not depended on the position of current density. These values can be calculated by Eq D3 and D4. (Achenbach, 1994)

$$\tilde{R}_{pol,c,O_2} = \left[\frac{4F}{RT} k_{O_2} (x_{O_2,c})^{m_{O_2}} \exp\left(-\frac{E_{A,pol,O_2}}{RT}\right) \right]^{-1} \quad (D3)$$

$$\tilde{R}_{pol,a,H_2} = \left[\frac{2F}{RT} k_{H_2} (x_{H_2,a})^{m_{H_2}} \exp\left(-\frac{E_{A,pol,H_2}}{RT}\right) \right]^{-1} \quad (D4)$$

Where each constant values are shown in Table D2.

Table D2 Constant used for the cathode and anode polarization resistance

	k (A/m ²)	E _{A,pol} (J/mol K)	m
\tilde{R}_{pol,c,O_2}	14.9 × 10 ⁹	160 × 10 ³	0.25
\tilde{R}_{pol,a,H_2}	0.213 × 10 ⁹	110 × 10 ³	0.25

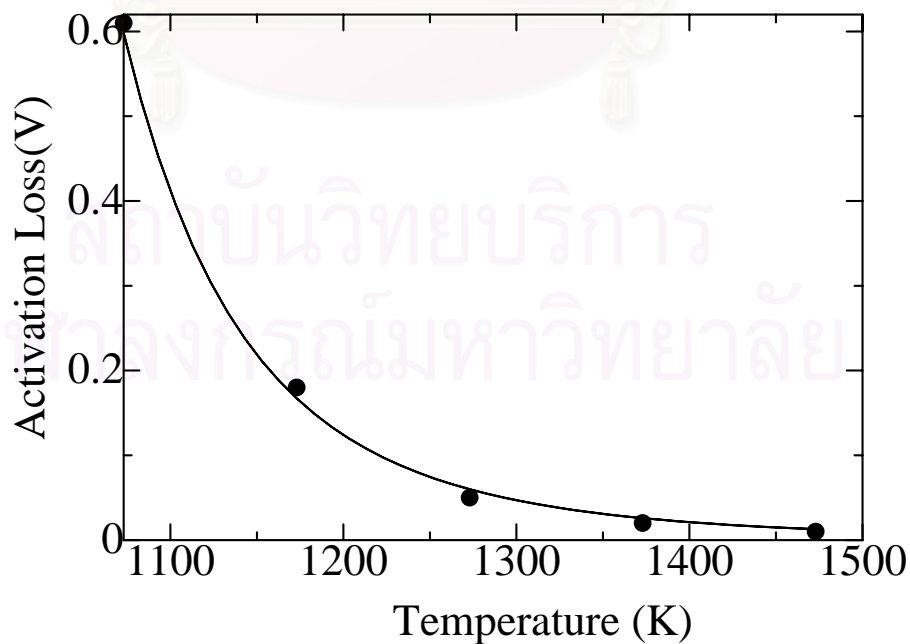


Fig. D1. Total activation overpotential using Achenbach at current density 3000 A/m²

Table D3 Total activation overpotential using Achenbach at 3000A/m² from literature (Pacheco *et al.*, 2004).

Temperature (K)	Activation Polarization (V)
	Achenbach
1073	0.62
1173	0.18
1273	0.05
1373	0.02
1473	0.01

A comparison between these correlations and the Butler–Volmer equation reveals that the empirical correlations were reasonably accurate between 1073 and 1473 K. At higher temperatures, the empirical expressions gave polarization values much smaller than the Butler–Volmer equation, which was expected based on the assumptions used for these correlations. However, at lower and higher temperatures ($T \leq 1173$ K and $T \geq 1473$ K), the numerical values reported unrealistic results and cannot be used for any practical purpose. Thus Achenbach correlation has accurate data at 1173 K (Pacheco *et al.*, 2004).

สถาบันวิทยบริการ
จุฬาลงกรณ์มหาวิทยาลัย

APPENDIX E

PALLADIUM MEMBRANE REACTOR

The ability of hydrogen transfer through palladium membrane is typically quantified in term of permeability, performance of flux. The *flux* of hydrogen through palladium membrane is the product of the diffusion coefficient and concentration gradient, with the flux of hydrogen atoms being twice that of hydrogen molecular:

$$N_H = 2N_{H_2} = -D_M \frac{\Delta n_H}{\delta} \quad (E1)$$

In assumption, the surface reaction is considered to be very fast and dissolved hydrogen atoms at the surface of the palladium are in equilibrium with the hydrogen gas on either side of membrane. The concentration of hydrogen atoms in the palladium can be related to the hydrogen partial pressure via the *Sievert's equation*. The exponent of 0.5 reflects the dissociation of the gaseous hydrogen molecule into two hydrogen atoms that diffuse into the metal, where an ideal solution of hydrogen atoms in palladium is formed:

$$n_H = K_s p_{H_2}^{0.5} \quad (E2)$$

The hydrogen permeability of palladium corresponds to the constant in Eq. E1 and E2. It is one half of product of the diffusion coefficient and the *Sieverts* constant.

$$k = \frac{1}{2} D_M K_s \quad (E3)$$

The temperature dependence of permeability values was calculated with an *Arrhenius* –type relation Eq. E3

$$k = Q_0 \exp\left(-\frac{E}{RT}\right) \quad (E4)$$

Therefore, the hydrogen flux is inversely proportional to the membrane thickness and directly proportional to the product of the hydrogen permeability and hydrogen partial pressure gradient across the membrane. Combining these expressions:

$$N_{H_2} = \frac{Q_0}{\delta} \exp\left(\frac{-E_D}{RT}\right) (P_{H_2,r}^{0.5} - P_{H_2,p}^{0.5}) \quad (\text{E5})$$

Where N_{H_2} is molar flux of hydrogen

Q_0 is pre-exponential constant for membrane permeability

E_D is activation energy for diffusion through membrane

δ is thickness of membrane

Table E1 Regressed parameter for the diffusion of hydrogen through Pd membrane

	Q_0 (mol m ⁻¹ s ⁻¹ Pa ^{-0.5})	E_D (kJ mol ⁻¹)	Thickness (μm)	Source
Palladium	4.40x10 ⁻⁷	15.7	10	Holleck (1970)

APPENDIX F

LIST OF PUBLICATIONS

International Publications

- 1) S. Assabumrungrat, N. Laosiripojana, V. Pavarajarn, W. Sangtongkitcharoen, A. Tangjitmatee, P. Prasertthdam; "Thermodynamic analysis of carbon formation in a solid oxide fuel cell with a direct internal reformer fuelled by methanol," *Journal of Power Sources*, 139, 55–60 (2005).
- 2) S. Assabumrungrat, W. Sangtongkitcharoen, N. Laosiripojana, A. Arpornwichanop, S. Charojrochkul, P. Prasertthdam; "Effects of electrolyte type and flow pattern on performance of methanol-fulled solid oxide fuel cells," *Journal of Power Sources*, 148, 18–23 (2005).

International Conferences

- 1) W. Sangtongkitcharoen, S. Assabumrungrat, V. Pavarajarn, N. Laosiripojana and P. Prasertthdam; "Prediction of Boundary of Carbon Formation for Different Types of Solid Oxide Fuel Cells with Methane Feed," *Regional Symposium on Chemical Engineering (RSCE 2004)*, Bangkok, December 1-3, 2004 (oral presentation).
- 2) W. Sangtongkitcharoen, S. Assabumrungrat, N. Laosiripojana, A. Arpornwichanop, and P. Prasertthdam; "Benefit of incorporating palladium membrane reactor in methanol-fueled solid oxide fuel cell system," 6th *International Symposium on Catalysis in Multiphase Reactor (CAMURE-6)* & 5th *International Symposium on Multifunctional Reactor (ISMR-5)*, New deli, India, 2006 (oral presentation) (waiting for acceptance).

VITA

Mr. Wiboon Sangtongkitcharoen was born in September 27th, 1981 in Bangkok, Thailand. He finished high school from Debsirin School, Bangkok in 2000, and received bachelor's degree in Chemical Engineering from department of Chemical Engineering, Faculty of Engineering, Chulalongkorn University, Bangkok, Thailand in 2004.



สถาบันวิทยบริการ
จุฬาลงกรณ์มหาวิทยาลัย